RESONANCE LINE ABSORPTION METHOD FOR DETERMINATION OF NITRIC OXIDE CONCENTRATION

W. K. McGregor and J. D. Few

ARO, Inc.

and

C. D. Litton

The University of Tennessee Space Institute

December 1973

ENGINE TEST FACILITY

ARNOLD ENGINEERING DEVELOPMENT CENTER

AIR FORCE SYSTEMS COMMAND

ARNOLD AIR FORCE STATION, TENNESSEE

NOTICES

When U. S. Government drawings specifications, or other data are used for any purpose other than a definitely related Government procurement operation, the Government thereby incurs no responsibility nor any obligation whatsoever, and the fact that the Government may have formulated, furnished, or in any way supplied the said drawings, specifications, or other data, is not to be regarded by implication or otherwise, or in any manner licensing the holder or any other person or corporation, or conveying any rights or permission to manufacture, use, or sell any patented invention that may in any way be related thereto.

Qualified users may obtain copies of this report from the Defense Documentation Center.

References to named commercial products in this report are not to be considered in any sense as an endorsement of the product by the United States Air Force or the Government.

RESONANCE LINE ABSORPTION METHOD FOR DETERMINATION OF NITRIC OXIDE CONCENTRATION

W. K. McGregor and J. D. Few
ARO, Inc.

and

C. D. Litton
The University of Tennessee Space Institute

FOREWORD

The research reported here was conducted at Arnold Engineering Development Center (AEDC), Air Force Systems Command (AFSC), and was carried out under sponsorship of the USAF Aerospace Research Laboratories, Wright-Patterson AFB, Ohio, under Program Element 65802F.

The results of this research program were obtained by ARO, Inc. (a subsidiary of Sverdrup & Parcel and Associates, Inc.), contract operator of AEDC, AFSC, Arnold Air Force Station, Tennessee. The experiments were performed in Propulsion Research Area (R-2E) of the Engine Test Facility (ETF) under ARO Project number RW5211, and the manuscript was submitted for publication on August 16, 1973.

The authors extend acknowledgement to Mr. Bryan L. Seiber, ARO, Inc., Propulsion Wind Tunnel (PWT), and to Dr. Arthur A. Mason, The University of Tennessee Space Institute (UTSI), for helpful discussions which contributed materially to this work, and to Mr. Howard Glassman, who wrote the computer code for simulation of the spectra.

This technical report has been reviewed and is approved.

MARION L. LASTER
Research and Development Division
Directorate of Technology

ROBERT O. DIETZ
Director of Technology

ABSTRACT

The details of the derivation of working equations for the determination of the concentration of nitric oxide for measurement of the absorption of individual spectral lines lying between 2270 and 2260 Å in the NO (0,0) γ-band are presented. It is shown experimentally that the derivation is accurate, that published values of oscillator strengths are adequate, and that measurements of number densities with uncertainty no greater than ±20 percent are possible when proper corrections for the relative line widths of source and absorber are made. The density range of use of the (0,0) γ-band is from about 10^{14} to 10^{16} cm^{-3} for path lengths usually encountered in combustion system testing (10 to 100 cm). Extension of the range to larger concentrations by use of the (0,1) γ-band and the application to media having nonuniform concentration and temperature are discussed.

CONTENTS

ILLUSTRATIONS

NOMENCLATURE

α	Absorptivity of radiation by a medium
ν	Frequency, cm^{-1}
I^o	Incident radiation intensity, arbitrary but consistent units
I_m	Measured radiation intensity, arbitrary but consistent units
t_ν	Transmissivity of radiation through a medium at frequency, ν
$\Delta\nu$	Frequency interval, cm^{-1}
k_ν	Absorption coefficient at frequency, ν, cm^{-1}

ℓ	Path length, cm
I_ν	Radiation intensity at frequency, ν, arbitrary units
I_ν^o	Incident radiation intensity at frequency, ν, arbitrary units
k_{ν_o}	Absorption coefficient at line center frequency, ν_o, cm^{-1}
I_m^o	Measured source intensity, arbitrary units
L	Total path length, cm
I_{ν_o}	Radiation intensity at line center frequency, ν_o, arbitrary units
t_m	Measured transmissivity of radiation through a medium
J''	Rotational angular momentum quantum number of lower state
J'	Rotational angular momentum quantum number of upper state
$A_{J'J''}$	Probability of a spontaneous radiating transition from quantum state J' to quantum state J'', sec^{-1}
$N_{J'}, N_{J''}$	Number of molecules in quantum state J' and quantum state J'', respectively, molecules/cm^3
$B_{J'J''}$	Probability per unit radiation intensity at frequency ν of an induced radiating transition from quantum state J' to quantum state J'', sec^{-1}/intensity unit
$B_{J''J'}$	Probability per unit radiation intensity at frequency ν of an induced absorbing transition from quantum state J'' to quantum state J', sec^{-1}/intensity unit
h	Planck's constant, 6.625×10^{-27} erg sec
c	Velocity of light, 3×10^{10} cm/sec
$g_{J''}, g_{J'}$	Statistical weights of the lower and upper quantum states, respectively
$N_{\nu_{J''}}, N_{\nu_{J'}}$	Number of molecules capable of absorbing a photon of frequency ν or emitting a photon of frequency ν, respectively, molecules/cm^3
$E_{J''}, E_{J'}$	Potential energy of the lower J'' quantum state and the upper J' quantum state, respectively, cm^{-1}
κ	Boltzmann's constant, 0.6952 $cm^{-1}/°K$

T	Temperature, °K
e	Charge on the electron, 4.803×10^{-10} esu
$f_{J'J''}$	Oscillator strength for a spectral line corresponding to a transition from the J′ to the J″ quantum state
$\Delta\nu_D$	Half-width of an emission or absorption line due to Doppler broadening, cm^{-1}
M	Mass of molecule, gm
t_{ν_o}	Transmission at line center frequency, ν_o
y	Distance from axis of cylinder, cm
r	Radius of cylinder, at any value y, cm
R	Radius of cylinder, cm
$\mathcal{T}_e$	Term energy of an electronic state, cm^{-1}
$G(v)$	Vibrational energy of the vth quantum state, cm^{-1}
$F(J'')$	Rotational energy of the J″th quantum state, cm^{-1}
S	Electron spin angular momentum quantum number
N_o	Total number density of absorbing species, molecules/cm^3
Q_e, Q_v, Q_R	Electronic, vibrational, and rotational partition functions, respectively
$f_{J'J''}$	Oscillator strength of a single transition from the J′ rotational state of the upper electronic-vibrational level to the J″ rotational state of the lower electronic-vibrational level
$f_{v'v''}$	Oscillator strength for all rotational transitions from the v′ vibrational level to the v″ vibrational level
$f_{e\ell}$	Electronic oscillator strength
$q_{v'v''}$	Vibrational overlap integral, or Franck-Condon factor
$\lambda_{v'v''}$	Wavelength at the bandhead of the (v′,v″) band, cm
$\lambda_{J'J''}$	Wavelength of a particular (J′J″) line in the (v′, v″) band, cm
$\delta_{J'J''}$	Rotational line strength or Hönl-London factor
ω_e	First vibrational constant, cm^{-1}
$\omega_e x_e$	Second vibrational constant, cm^{-1}

$\omega_e y_e$	Third vibrational constant, cm^{-1}
K	Rotational angular momentum quantum number
B_v	First rotational constant, cm^{-1}
D_v	Second rotational constant, cm^{-1}
α_e	Third rotational constant, cm^{-1}
β_e	Fourth rotational constant, cm^{-1}
$F_n(J)$	Rotational energy of the Jth quantum state, n = 1, $F_1(J - 1/2)$ and n = 2, $F_2(J + 1/2)$, cm^{-1}
u	Function used in Hill and van Fleck formula
Y_v	Constant used in Hill and van Fleck formula
A	Uncoupling constant for states intermediate between Hund's coupling cases (a) and (b)
Γ	Splitting constant for states in Hund's coupling case (b)
U	Function used in Hönl-London factor expressions for states intermediate between Hund's cases (a) and (b)
C	Defined constant used in final equation relating number density of molecules to the measured absorption coefficient
a	Ratio of the line width of the radiation source to the line width of the absorbing gas
W	Defined function of frequency
λ	Wavelength, cm

SECTION I
INTRODUCTION

A large effort is currently being put forth to measure the contribution to atmospheric pollution of nitric oxide (NO) for automobile and jet engine exhausts. Techniques used to measure NO concentrations have generally been hindered by (1) the small concentrations which are encountered in pollution sources (on the order of 100 parts per million), and (2) the tendency of NO to chemically combine with other compounds in sample cells and hence reduce the actual concentration in the sample measured. No completely satisfactory method has been developed to measure NO concentrations. Reported herein are the results of an investigation of the feasibility of a nonsampling, in situ, ultraviolet absorption method to measure NO concentrations.

The specific purpose of the work reported herein was to develope a technique to determine concentrations of NO from measurement of the absorption of spectral lines lying in the ultraviolet γ-bands of NO. The narrow line absorption technique has been in use for many years but application to the NO molecule has not been made, principally because of the inability of ordinary spectrometric equipment to completely resolve the rotational lines in the NO γ-bands. A lucid explanation of the spectral line absorption technique is contained in the book by Mitchel and Zemansky (Ref. 1) but certain adjustments must be made in order to apply the technique to the NO molecule. The development of the theory of absorption of spectral lines will be systematically made in this report for the sake of clarity, although portions of the treatment appear throughout the literature. Other research programs at AEDC (Refs. 2 and 3) have made use of the narrow line absorption method for determination of hydroxyl (OH) concentrations in flames, but the treatment of the equations for OH is not quite the same as for NO because of the different molecular structure and line broadening properties. Tabulations of the structural properties of the NO molecule are also scattered in the literature, and these data will also be assembled in a systematic manner in this report. Finally, a numerical working equation for determination of NO concentration from measured spectral line transmission will be developed.

In the experimental work, a high-intensity, narrow-line source of NO radiation was developed. Parallel light emanating from the source was passed through a cylindrical absorption cell containing NO at a known partial pressure. The length of the absorption cell was

accurately known, and the diameter of the beam of parallel light passing through the cell was smaller than the diameter of the absorption cell. The concentration of NO as determined from measurements of the temperature and pressure in the absorption cell was compared with the results of the absorption measurement. The results of the comparison were satisfactory, considering the uncertainties in the theory and the measurements. Finally, some implied conclusions about the method, the development of the theory, and applications are discussed.

SECTION II
THEORY OF THE METHOD

2.1 DESCRIPTION OF THE MEASUREMENT PROCEDURE

The basic principle upon which the measurement technique being described here exists is that a beam of light is absorbed by the gas at some determinable wavelength, and that the magnitude of the absorption is uniquely related to the concentration and temperature of the absorbing species along the path length. The measurement required is the absorptivity

$$\alpha_\nu = [(I^\circ - I_m)/I^\circ]_\nu$$

or transmissivity

$$t_\nu = [I_m/I^\circ]_\nu$$

within a given wave number interval ($\Delta\nu$) where I° is the incident intensity and I_m is the transmitted intensity as illustrated in Fig. 1. The problem is to relate this measurement to the properties (concentration of absorbing species, temperature, and pressure) of the absorbing medium. This section is devoted to a systematic derivation of the relationship between the measured transmission and the concentration and temperature of the NO molecule and the pressure of the absorbing medium.

The (0,0) band of the ultraviolet resonance γ-system of NO was chosen for the measurements. The first band-head of the (0,0) band is at 2269.4 Å. NO has an infrared absorption spectrum at about 5.2 microns, but this region of the spectrum is cluttered with band systems of other molecules such as CO and several minor components of

combustion gases. The 2269 Å region does not suffer from overlapping of other bands.

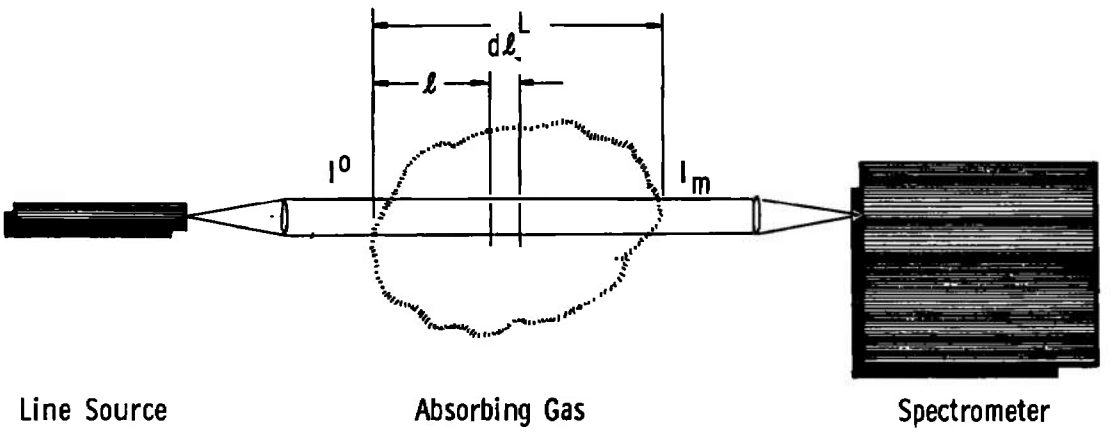

Fig. 1 Physical Arrangement for Spectral Line Absorption Measurements

2.2 DEFINITION OF THE ABSORPTION COEFFICIENT

If radiation from a continuum source is directed through a gas as shown in Fig. 1, the transmitted beam will suffer absorption at selected wave numbers appropriate to the gas species. The absorption coefficient (k_ν) of the gas at some appropriate wave number (ν) is defined by the equation (Ref. 1):

$$\frac{dI_\nu}{d\ell} = -k_\nu I_\nu \tag{1}$$

where I_ν is the intensity of a beam of light of wave number (ν) at a distance (ℓ) into the gas, and dI_ν is the decrease in intensity after passing through a thickness ($d\ell$) of the gas. If the gas has uniform properties, then k_ν will be independent of the position and Eq. (1) may be integrated to give

$$\frac{I_\nu}{I_\nu^o} = \exp(-k_\nu L) \tag{2}$$

where I_ν^o is the incident intensity at wave number (ν) at the entrance to the absorbing layer of thickness (L). If the properties are not uniform,

then

$$\frac{I_\nu}{I_\nu^o} = \exp\left(-\int k_\nu d\ell\right) \tag{3}$$

For a real gas, the absorption coefficient of an absorption line is a function of the frequency or wave number; that is, the envelope of the transmission $((I/I^o)_\nu)$ and the absorption coefficient (k_ν) of a continuum source will have the approximate shapes shown in Fig. 2a. The total width of the absorption coefficient curve at the frequency where k_ν has fallen to one-half of k_{ν_o}, its maximum value, is called the half-width of the absorption line and is denoted as $\Delta\nu$. In general, the absorption coefficient of a gas is given by an expression involving a function of ν and a definite value of k_{ν_o} and $\Delta\nu$, both of which are functions of the local gas pressure and temperature.

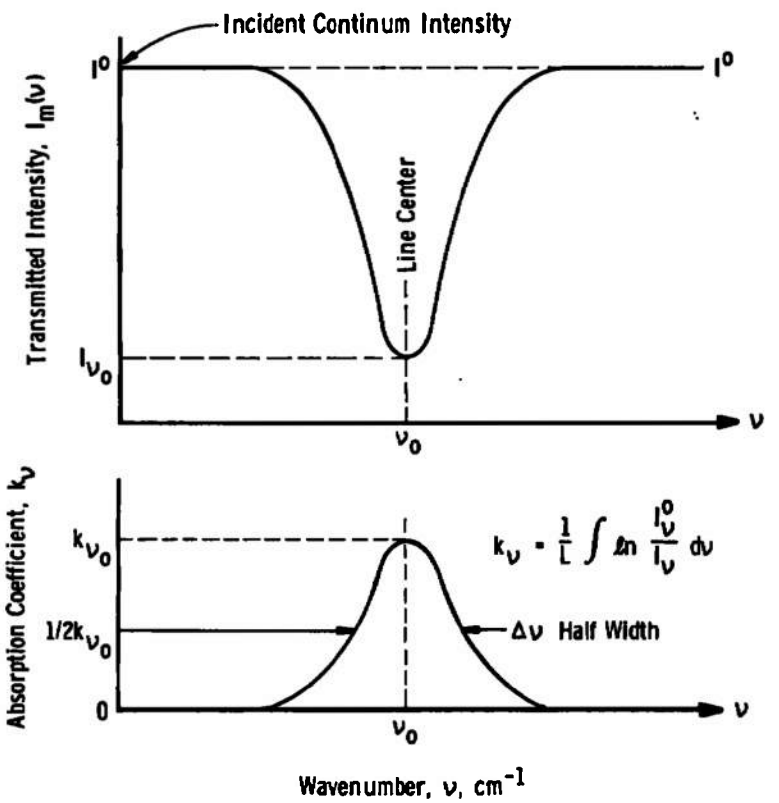

a. Continuum Intensity Source

Fig. 2 Transmitted Intensity and Absorption Coefficient in an Absorbing Gas

In most practical cases in the ultraviolet portion of the spectrum, $\Delta\nu$ is much smaller than the band-pass of the instruments that must be used, so that it is the integral over frequency that is measured:

$$I_m = \int_0^\infty I_\nu^o \exp(-k_\nu L)d\nu \tag{4}$$

If the source is a continuum, then I_{ν_o} is a constant and may be removed from the integral:

$$I_m = I^o \int_{2\Delta\nu} \exp(-k_\nu L)d\nu \tag{5}$$

and the transmission ($t_m = (I_m/I^o)$) is a measure of the absorption integral.

Now, suppose the source is not a continuum but a line at the same frequency as the absorption line but much narrower, as illustrated in Fig. 2b. Then, absorption takes place only over the extent of the incident radiation:

$$I_m = \int_{2\Delta\nu} I_\nu^o \exp(-k_\nu L)d\nu \tag{6}$$

But now k_ν is just the absorption at line center (k_{ν_o}) and is constant over the integral:

$$I_m = \exp(-k_{\nu_o} L)\int_{2\Delta\nu} I_\nu^o d\nu = I_{\nu_o}^o \exp(-k_{\nu_o} L) \tag{7}$$

This latter expression is much simpler than Eq. (5) and does not depend on the line shape. This is the essence of the narrow line absorption technique. Furthermore, the measured transmission ($t_m = I_m/I_{\nu_o}^o$) is a sensitive function of k_{ν_o}.

Suppose that the incident line is not much narrower than the absorption line. The measured transmission is not now a simple function of the absorption coefficient as in the cases defined by Eqs. (5) and (7). Rather, the relationship becomes

$$t_m = \frac{I_m}{I_m^o} = \frac{\int I_\nu d\nu}{\int I_\nu^o d\nu} = \frac{\int I_\nu^o \exp(-k_\nu L)d\nu}{\int I_\nu^o d\nu} \tag{8}$$

involving the details of the incident source variation with wave number and the absorption line shape. This is the more general line absorption problem and, although much more difficult because of the integration problems, is still much more sensitive to a change in k_ν than the continuum expression (Eq. (5)).

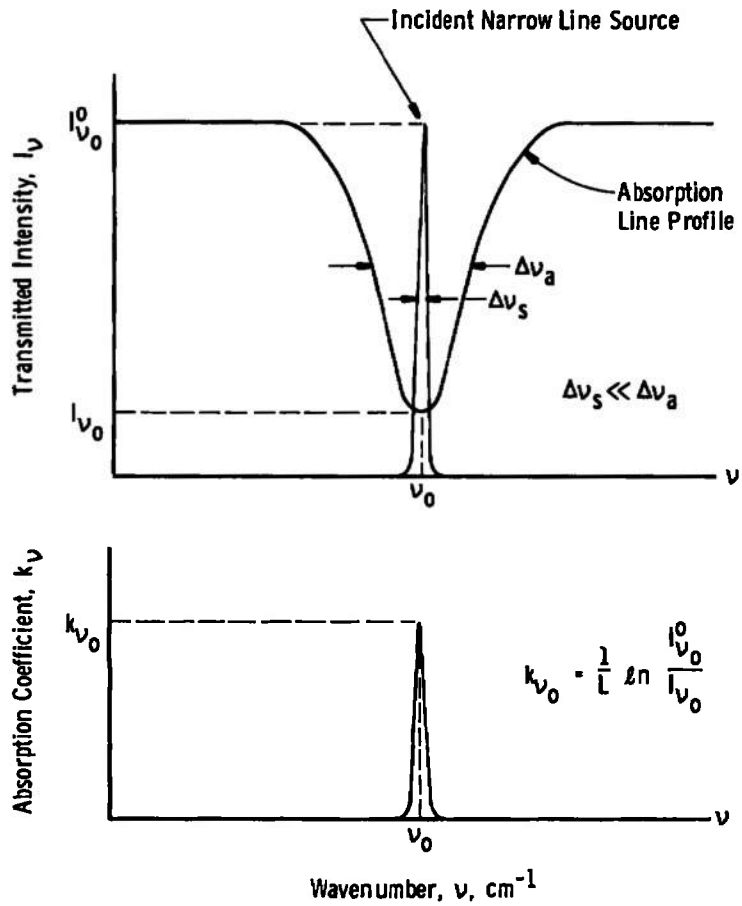

b. Narrow Line Source
Fig. 2 Concluded

The problem is, then, to determine means by which the measured transmission may be related to the properties of the gas, which are expressible through $\int k_\nu d\nu$. In the following sections, the relationship between $\int k_\nu d\nu$ and the gas temperature, pressure, and concentration of the absorbing species will be developed, and by examination of the details of the function (k_ν) means will be found to extract $\int k_\nu \, d\nu$ from the measured transmission.

2.3 EINSTEIN EQUATION FOR RADIATION

First, consider the situation in which an enclosure contains isotropic radiation of wave number between ν and $\nu + d\nu$, intensity I_ν, and molecules capable of being raised by absorption of the radiation from the rotational state J'' of one-electronic-vibrational level to the state J' of some higher electronic-vibrational level. The Einstein radiation law relates the rate of photon production from a unit volume of gas for a given transition, to the properties of the gas (Ref. 1); that is, the rate of photon production is equal to

$$A_{J'J''}N_{J'} + B_{J'J''}\frac{I_\nu}{4\pi}N_{J'} - B_{J''J'}\frac{I_\nu}{4\pi}N_{J''} \tag{9}$$

where the Einstein transition probabilities are defined by Milne as described in Ref. 1 in terms of intensity as follows:

1. $B_{J''J'}I_\nu$ = probability per second that the molecule in state J'' exposed to isotropic radiation of wave number between ν and $\nu + d\nu$ and intensity, I_ν, will absorb a quantum $hc\nu$ and pass to the state J'. (h is Planck's constant and c is the velocity of light.)
2. $A_{J'J''}$ = probability per second that the molecule in state J' will spontaneously emit a quantum $hc\nu$ and pass to the state J''.
3. $B_{J'J''}I_\nu$ = probability per second that the molecule will undergo the transition from J' to J'' when it is exposed to isotropic radiation of wave number between ν and $\nu + d\nu$ and intensity, I_ν, and emit a quantum $hc\nu$.

The Einstein transition probabilities as used in Eq. (9) are related by the following equations (Ref. 1):

$$\frac{A_{J'J''}}{B_{J''J'}} = 2hc\nu^3\frac{g_{J''}}{g_{J'}} \tag{10}$$

$$\frac{B_{J'J''}}{B_{J''J'}} = \frac{g_{J''}}{g_{J'}} \tag{11}$$

where $g_{J''}$ and $g_{J'}$ are the statistical weights of the lower and upper excited states, respectively.

Consider a parallel beam of light of wave number between ν and $\nu + d\nu$ and traveling in the positive direction through a layer of molecules bounded by the planes at ℓ and $\ell + d\ell$ (Fig. 1). Suppose there are $N_{J''}$ molecules per cubic centimeter in the J'' state of which $\delta N_{\nu J''}$ are capable of absorbing in the range between ν and $\nu + \delta\nu$, and $N_{J'}$ excited molecules per cubic centimeter in the J' state of which $\delta N_{\nu J'}$ are capable of emitting in this wave number interval. Assuming that the incident intensity is much greater than the spontaneous emission, the first term on the right of Eq. (9) can be neglected and the decrease in intensity of the incident beam along the path is given by

$$-d[I_\nu \delta_\nu] = \delta N_{\nu J''} h\nu B_{J''J'} \frac{I_\nu}{4\pi} d\ell - \delta N_{\nu J'} h\nu B_{J'J''} \frac{I_\nu}{4\pi} d\ell \tag{12}$$

where $I_\nu / 4\pi$ is the intensity of the equivalent isotropic radiation for which $B_{J''J'}$ and $B_{J'J''}$ are defined. Rewriting Eq. (12) gives

$$-\frac{1}{I_\nu} \frac{dI_\nu}{d\ell} \delta\nu = \frac{h\nu}{4\pi} (B_{J''J'} \delta N_{\nu J''} - B_{J'J''} \delta N_{\nu J'}) \tag{13}$$

By recognizing that the left hand side of the equation is $k_\nu \delta\nu$ with k_ν as defined by Eq. (1), Eq. (13) becomes

$$k_\nu \delta\nu = \frac{h\nu}{4\pi} (B_{J''J'} \delta N_{\nu J''} - B_{J'J''} \delta N_{\nu J'}) \tag{14}$$

Integrating over the whole absorption line and neglecting the small change in ν throughout the line results in

$$\int k_\nu d\nu = \frac{h\nu_o}{4\pi} (B_{J''J'} N_{J''} - B_{J'J''} N_{J'}) \tag{15}$$

where ν_o is the wave number at the center of the line. By using Eqs. (10) and (11), Eq. (15) can be rewritten as

$$\int k_\nu d\nu = \frac{g_{J'}}{g_{J''}} \frac{A_{J'J''} N_{J''}}{8\pi c \nu_o^2} \left[1 - \frac{g_{J''} N_{J'}}{g_{J'} N_{J''}}\right] \tag{16}$$

For gases in equilibrium, the Boltzmann distribution holds, and

$$\frac{N_{\text{upper}}}{N_{\text{lower}}} = \frac{N_{J'}}{N_{J''}} = \frac{g_{J'}}{g_{J''}} \exp\left(\frac{E_{J''} - E_{J'}}{\kappa T}\right) \tag{17}$$

where $E_{J''}$ is the potential energy of the lower electronic vibrational-rotational state, $E_{J'}$ is the energy of the upper J′ state, κ is Boltzmann's constant, and T is the gas temperature. For the ultraviolet spectral region, $E_{J''} - E_{J'} \sim -40{,}000\ \text{cm}^{-1}$, $\kappa = 0.695\ \text{cm}^{-1}/°\text{K}$, and for the temperatures encountered (300 to 3000°K), the exponential is very small. Thus $N_{J'}/N_{J''} < 10^{-7}$, and the term in parenthesis in Eq. (16) is approximately unity. That is,

$$\int k_\nu d\nu = \frac{g_{J'}}{g_{J''}} \frac{N_{J''} A_{J'J''}}{8\pi c \nu_o^2} \tag{18}$$

The spontaneous transition probability ($A_{J'J''}$) is related to a term most used in the literature, the oscillator strength, or f-value, through the equation (Ref. 1):

$$\frac{\pi e^2}{mc^2} N_{J''} f_{J'J''} = \frac{g_{J'}}{g_{J''}} \frac{N_{J''} A_{J'J''}}{8\pi c \nu_o^2} \tag{19}$$

where m is the electron mass and e is the electron charge. Substituting Eq. (19) into Eq. (18) then gives

$$\int k_\nu d\nu = \frac{\pi e^2}{mc^2} N_{J''} f_{J'J''} \tag{20}$$

2.4 SPECTRAL LINE SHAPE

Equation (20) expresses the integral of the absorption coefficient in terms of the population density of the lower rotational state of the absorbing gas ($N_{J''}$) which is a function of the density of the absorbing species and the temperature, and $f_{J'J''}$, which is a constant of the molecule. However, an explicit expression for k_ν or $\int k_\nu d\nu$ in terms of the measured transmittance or absorption must be obtained in order to use this relationship. An examination of the processes that contribute to the formation of an absorption line of a gas will yield information leading to such an expression.

There are, in general, five processes which contribute to the definition of the shape of an absorption or emission line. Each process can

be regarded as an agent for perturbing the energy levels associated with the transition. The result is a broadening of the line. The five processes are:

1. Natural broadening, due to the finite lifetime of the excited state.
2. Doppler broadening, due to the motions of the molecules.
3. Lorentz broadening, due to collisions with foreign gases.
4. Holtsmark broadening, due to collisions with other absorbing molecules of the same kind.
5. Stark broadening, due to collisions with electrons and ions.

Processes 1 and 5 may be neglected for the temperature range being considered since they contribute much less to the broadening than processes 2, 3, and 4. Processes 3 and 4 have generally been grouped together under the name "pressure" broadening. Thorson and Badger (Ref. 4) have shown that pressure broadening in the bands of NO is much less than Doppler broadening at temperatures greater than room temperature and at pressures less than atmospheric. Therefore, for the work reported here, pressure broadening was neglected and to a very good approximation, Doppler broadening is the only process which contributes to the formation of absorption lines for the NO γ-bands. For the OH molecule, this is not the case,. and the combined Doppler and pressure broadening had to be considered (Refs. 2 and 3).

When Doppler broadening is the dominant mechanism the absorption coefficient is given by (Ref. 1):

$$k_\nu = k_{\nu_o} \exp\left[-\frac{2(\nu - \nu_o)}{\Delta\nu_D}\sqrt{\ell n\, 2}\right]^2 \tag{21}$$

where $\Delta\nu_D$ is the Doppler half-width at half of k_{ν_o}, the maximum absorption coefficient, and $\Delta\nu_D$ depends only on the absolute temperature (T), the central wave number (ν_o), and the molecular mass (M) of the absorbing species, according to the relation

$$\Delta\nu_D = 2\nu_o \frac{\sqrt{2\kappa T\, \ell n 2}}{mc^2} \tag{22}$$

Integrating Eq. (21) over ν yields the result

$$\int_0^\infty k_\nu d\nu = \tfrac{1}{2}\sqrt{\pi/\ell n 2}\, k_{\nu_o} \Delta\nu_D \tag{23}$$

Equating the right hand sides of Eqs. (20) and (23) gives

$$\tfrac{1}{2}\sqrt{\pi/\ell n 2}\, k_{\nu_o} \Delta\nu_D = \frac{\pi e^2}{mc^2} N_J'' f_{J'J''} \tag{24}$$

Now, rewriting Eq. (24) in terms of the absorption coefficient at the line center (k_{ν_o}), the Doppler width ($\Delta\nu_D$), and known properties of the molecule results in

$$N_J'' = \frac{1}{2\sqrt{\pi \ell n 2}} \frac{mc^2}{e^2} \frac{k_{\nu_o} \Delta\nu_D}{f_{J'J''}} \tag{25}$$

It should be noted at this point that the assumption of a Doppler line shape has imposed a very useful property for the measurement technique. In Eq. (25), N_J'' has been simply related to the absorption coefficient at line center (k_{ν_o}) so that some contrivance which enables this measurement to be made is a necessary part of the technique. Then, Eq. (7) is applicable, and k_{ν_o} can easily be determined experimentally.

The measurement can be accomplished if the source in Fig. 1 is composed of lines having the same wavelength as those of the species to be measured, which are very narrow compared with the width of the absorption lines. One way in which this may be accomplished is through use of a resonance lamp containing the species of interest in which the temperature of the source is much less than the temperature of the absorbing medium. Even when the source lines are of comparable width to those of the absorber, the integrals in Eq. (8) can be solved if the incident line shape and the absorption line shape are known. A solution of Eq. (8) for the case of Doppler line shapes is given in Appendix I where it is shown that the measured transmission can be expressed in terms of the line center transmission (t_{ν_o}).

A second feature of being able to express the integral of the absorption coefficient in terms of the absorption coefficient at line center is that the applicable measurement expression for variation of k_{ν_o} over the path is

$$t_m = \exp\left(-\int k_{\nu_o} d\ell\right) \tag{26}$$

where k_{ν_o} is a function of the density and temperature along the path as expressed in Eq. (25). This expression is now amenable to the geometric treatment of Abel inversion for axisymetric flow streams (Ref. 3). That is,

$$\ell n \frac{1}{t_m} = \int_L k_{\nu_o} d\ell \tag{27}$$

which, for an axisymetric source, can be inverted to (Ref. 3):

$$k_{\nu_o}(r) = -\frac{1}{\pi}\int_r^R \frac{\frac{d}{dy}(\ell n\, t_m^{-1})dy}{\sqrt{r^2 - y^2}} \tag{28}$$

where r is the radius, y is the distance from the axis where the measurement is made, and R is the full radius of the axisymetric source.

2.5 EQUATION FOR THE SPECIES CONCENTRATION

Under conditions of rotational equilibrium, Tatum (Ref. 5) gives expressions for the number density of diatomic molecules in a rotational-vibrational-electronic state satisfying Hund's case "b" as

$$\frac{N_{J''}}{N_o} = \left[\frac{2(2S+1)\exp(\mathcal{T}_e/\kappa T)}{\sum_{\substack{\text{all n}\\ \text{states}}} 2(2S+1)\exp(-\mathcal{T}_{e_n}/\kappa T)}\right]\left[\frac{\exp[-G(v'')/\kappa T]}{\sum_{\substack{\text{all v}\\ \text{states}}}\exp[-G(v'')/\kappa T]}\right]\left[\frac{(2J''+1)\exp[-F(J'')/\kappa T]}{(2S+1)\sum_{J''=0}^{\infty}(2J''+1)\exp[-F(J'')/\kappa T]}\right] \tag{29}$$

where the new terms used are defined as follows:

S is the electron spin angular momentum quantum number

$\mathcal{T}_e$ is the term energy of the electronic state

G(v″) is the vibrational energy of the ν″th vibrational state

F(J″) is the rotational energy of the J″th rotational state

N_o is the total number density of the absorbing species.

The first term in brackets goes to unity for a gas in which only the ground electronic state is populated as is the case in this study. The summations are usually identified as the partition functions for electronic,

$$Q_e = \sum_{o}^{\infty} 2(2S + 1) \exp [-\mathcal{T}_n/\kappa T] \quad . \tag{30}$$

vibration,

$$Q_v = \sum_{v=0}^{\infty} \exp [-G(v'')/\kappa T] \tag{31}$$

and rotation,

$$Q_R = \sum_{J''=0}^{\infty} (2J'' + 1) \exp [-F(J'')/\kappa T] \tag{32}$$

Substitution of Eq. (29) into Eq. (25) gives

$$\frac{N_o \exp [-G(v'')/\kappa T]}{Q_v Q_R} \frac{2J'' + 1}{2S + 1} \exp [-F(J'')/\kappa T] = \frac{1}{2\sqrt{\pi \ell n 2}} \frac{mc^2}{e^2} \frac{k_{\nu_o} \Delta\nu_D}{f_{J'J''}} \tag{33}$$

Rearrangement of terms in Eq. (33) then yields an equation for the total number density of the species:

$$N_o = \frac{mc^2/e^2}{\sqrt{4\pi\, \ell n 2}} \frac{Q_v}{\exp [-G(v'')/\kappa T]} \frac{2S + 1}{2J'' + 1} \frac{Q_R}{f_{J'J''} \exp [-F(J'')/\kappa T]} k_{\nu_o} \Delta\nu_D \tag{34}$$

Hence, if a single rotational line of known oscillator strength can be isolated and k_{ν_o} and T can be measured, the number density (N_o) of the absorbing species may be determined.

2.6 EXPRESSION FOR THE OSCILLATOR STRENGTH

The oscillator strength of a rotational line ($f_{J'J''}$) is defined throughout the literature in varying forms. The nomenclature, and hence consistent formulas for the calculation of rotational oscillator strengths, is a much confused subject. The definition of the oscillator strength as used by Schadee (Ref. 6) with the normalization used by Tatum (Ref. 5) will be used in this work. The vibrational oscillator strength ($f_{v'v''}$) is defined by

$$f_{v'v''} = f_{e\ell} q_{v'v''} \tag{35}$$

where $q_{v'v''}$ is the square of the vibrational overlap integral and is known as the Franck-Condon factor. For molecules for which vibrational constants have been accurately measured for several vibrational states, $q_{v'v''}$ can be accurately calculated. Most measurements of the oscillator strength give a value of a particular $f_{v'v''}$ so that f_e can then be found.

The rotational oscillator strength is given by

$$f_{J'J''} = f_{v'v''} \frac{\lambda_{v'v''}}{\lambda_{J'J''}} \frac{\delta_{J'J''}}{(2J''+1)(2)(2S+1)} \tag{36}$$

where $\lambda_{v'v''}/\lambda_{J'J''}$ is the ratio of the wavelength at the band head to the wavelength of the particular rotational line of interest. $\delta_{J'J''}/(2J''+1)$ is the normalized Hönl-London Factor for which Earls (Ref. 7) and Kovacs (Ref. 8) give formulas for most transitions encountered. Now, substituting Eq. (36) into Eq. (34) gives

$$N_o = \frac{mc^2/e^2}{\sqrt{4\pi \ell n 2}} \frac{2(2S+1)^2 Q_v Q_r}{\exp[-G(v'')/\kappa T]} \frac{\lambda_{J'J''}}{\lambda_{v'v''}} \frac{k_{\nu_o} \Delta\nu_D}{\delta_{J'J''} \exp[-F(J'')/\kappa T]} \tag{37}$$

which is the general working equation for narrow line absorption.

SECTION III
APPLICATION TO THE NO MOLECULE

A considerable amount of literature exists on the energy level structure of the NO molecule. This section is devoted to the definition of the energy levels and transition probabilities of the NO molecule applicable to this study.

3.1 ENERGY LEVELS

The ground electronic energy level of the NO molecule is a doublet Π state, denoted by $X\,{}^2\Pi$. All the upper electronic energy levels which have been observed are also doublet states and are denoted by $A\,{}^2\Sigma^+$, $B\,{}^2\Pi$, $C\,{}^2\Sigma^+$, $D\,{}^2\Sigma^+$, and $E\,{}^2\Sigma^+$ in order of increasing energy. The electronic transitions that have been observed are listed as follows (Ref. 9):

Transition	Designation
$A\ ^2\Sigma^+ \rightarrow X\ ^2\Pi$	γ system
$B\ ^2\Sigma^+ \rightarrow X\ ^2\Pi$	β system
$C\ ^2\Sigma^- \rightarrow X\ ^2\Pi$	δ system
$D\ ^2\Sigma^+ \rightarrow X\ ^2\Pi$	ϵ system

The energy level diagram showing the electronic energy levels and the transitions to the ground state, producing the γ, β, δ, and ϵ band systems, is shown in Fig. 3.

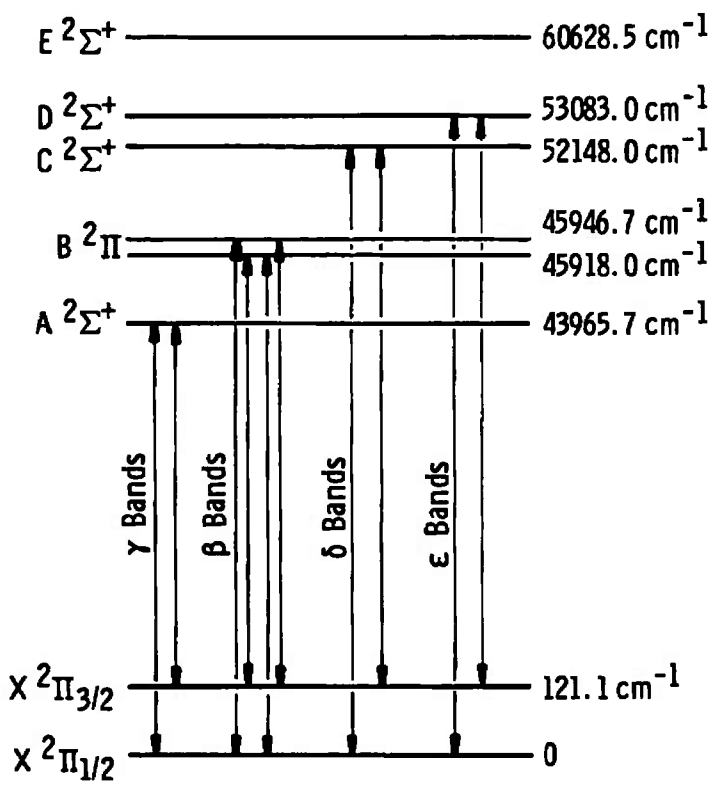

Fig. 3 Electronic Energy Level Diagram of NO Molecule Indicating the Various Band Systems

The applicable equations for determining the various vibrational and rotational energy levels and the vibrational and rotational constants for the NO molecule are given generally by Herzberg (Ref. 10). The majority of work with the NO molecule has dealt with the γ and β systems. Gero and Schmid (Ref. 9) have listed frequencies for

rotational lines in several bands of the γ and β systems and Deezsi (Ref. 11) has published a more comprehensive analysis of the Gero and Schmid data. Additionally, Gero, Schmid, and Von Szily (Ref. 12) give excellent data for the ϵ system and also locate rotational lines for a number of bands in this system. For the present work, the γ band system of NO was chosen because the wavelength region (2200 to 2400 Å) is more easily accessible than for the other, shorter wavelength bands and because the molecular constants are known more accurately.

In general, the equation for the energy levels of a given electronic energy term has the form

$$\mathcal{T} = \mathcal{T}_e + G(v) + F_n(J) \tag{38}$$

for which $\mathcal{T}_e$ is the ground state electronic energy for that level, G(v) includes the vibrational terms, and $F_n(J)$, the rotational terms.

G(v) has the form,

$$G(v) = \omega_e(v+\tfrac{1}{2}) - \omega_e x_e(v+\tfrac{1}{2})^2 + \omega_e y_e(v+\tfrac{1}{2})^3 + \cdots \tag{39}$$

where ω_e, $\omega_e x_e$, and $\omega_e y_e$ are vibrational constants (Ref. 10). Values of $\mathcal{T}_e$ and the vibrational constants for the A $^2\Sigma^+$ and X $^2\Pi$ states are given in Table I. Note in Table I that ω_e, as given by Gillette and Eyster (Ref. 13), is slightly different for the X $^2\Pi_{1/2}$ and X $^2\Pi_{3/2}$ states.

For doublet states, the term F_n refers to the two electron spin components, $F_1(K - 1/2)$ and $F_2(K + 1/2)$. The ground electronic energy level (X $^2\Pi$) is intermediate between Hund's cases (a) and (b) (Ref. 13). The Hill and Van Fleck equation for the rotational energy levels for the intermediate case as expressed by Churchhill, Hagstrom, and Landshoff (Ref. 14) is applicable to the X $^2\Pi$ state:

$$F_n(J'') = B_v[(J''+\tfrac{1}{2})^2 - 1 + (-1)^n u] - \begin{cases} D_v J''^4 & n = 1 \\ D_v(J''+1)^4 & n = 2 \end{cases} \tag{40}$$

where

$$B_v = B_e - \alpha_e(v+\tfrac{1}{2}) \tag{41}$$

$$D_v = D_e + \beta_e(v+\tfrac{1}{2}) \tag{42}$$

$$U = [(J''+\tfrac{1}{2})^2 - Y_v(1 - Y_v/4)]^{\frac{1}{2}} \tag{43}$$

$$Y_v = A/B_v \tag{44}$$

The constants (B_e, α_e, D_e, β_e, and A) for these equations as given in Ref. 13 are included in Table I.

TABLE I
MOLECULAR CONSTANTS USED TO CALCULATE SPECTRAL LINE WAVELENGTHS AND INTENSITIES FOR THE NO γ-BANDS

Molecular Constants, cm^{-1}	$X\ ^2\Pi_{1/2}$	$X\ ^2\Pi_{3/2}$	$A\ ^2\Sigma$
$\mathcal{T}_e$	62.1	62.1	43965.7
ω_e	1904.03	1903.68	2374.8
$\omega_e x_e$	13.97	13.97	16.46
$\omega_e y_e$	negligible	negligible	negligible
B_e	1.7046	1.7046	1.9972
α_e	0.0178	0.0178	0.01928
D_e	5×10^{-6}	5×10^{-6}	negligible
β_e	negligible	negligible	negligible
Γ	---	---	negligible
A	124.2	124.2	---
Ref.	13	13	15

The upper electronic energy level ($A\ ^2\Sigma^+$) of the γ-system belongs to Hund's case (b) as do all Σ states (Ref. 10). The equations for the rotational energy levels of $A\ ^2\Sigma^+$ states are given by Ref. 10 as

$$F_1(J') = B_v(J'-\tfrac{1}{2})(J'+\tfrac{1}{2}) + \tfrac{1}{2}\Gamma(J'-\tfrac{1}{2}) - D_v(J'-\tfrac{1}{2})^2(J'-\tfrac{1}{2})^2 \quad (45)$$

$$F_2(J') = B_v(J'+\tfrac{1}{2})(J'+\tfrac{3}{2}) - \tfrac{1}{2}\Gamma(J'+\tfrac{3}{2}) - D_v(J'+\tfrac{1}{2})^2(J'-\tfrac{3}{2})^2 \quad (46)$$

where $F_1(J')$ refers to the components with $J' = K' + 1/2$, and $F_2(J')$ refers to the components with $J' = K' - 1/2$. The splitting constant is Γ and, for NO, may be assumed negligible compared with B_v. The other constants for the $A\ ^2\Sigma^+$ level as derived from rotational analysis by Barrow and Miescher (Ref. 15) are given in Table I.

3.2 SPECTRAL LINES IN THE γ-SYSTEM

The energy of a transition between two levels of a band system is expressed by

$$\nu = \mathcal{T}(v', J') - \mathcal{T}(v'', J'') \tag{47}$$

The selection rules ($\Delta\nu = \nu' - \nu'' = 0, 1, 2, \ldots$ and $\Delta J = J' - J'' = 0, \pm 1$) apply to Eq. (47). By convention, branches of the band for which $\Delta J = 0$ are designated Q branches; for $\Delta J = +1$ they are R branches, and for $\Delta J = -1$ they are P branches. As noted earlier, both electronic energy levels of the system are split into an F_1 and an F_2 level. Because of this, there are then 12 possible transitions which will obey the selection rule. The 12 possible transitions to some J'' level in the $v = 0$ vibrational level of the $X\ ^2\Pi_{1/2,3/2}$ state are illustrated in Fig. 4. The designation of the various possible transitions shown in Fig. 4 consists of labeling the line as the P, Q, or R branch with subscripts which designate the F_1' or F_2' transition to the appropriate F_1'' or F_2'' rotational state. That is, $P_{11}(J'')$ refers to a transition from $F_1'(J'' - 1)$ to $F_1''(J'')$, $R_{21}(J'')$ refers to a transition from $F_2'(J'' + 1)$ to $F''(J'')$, etc.

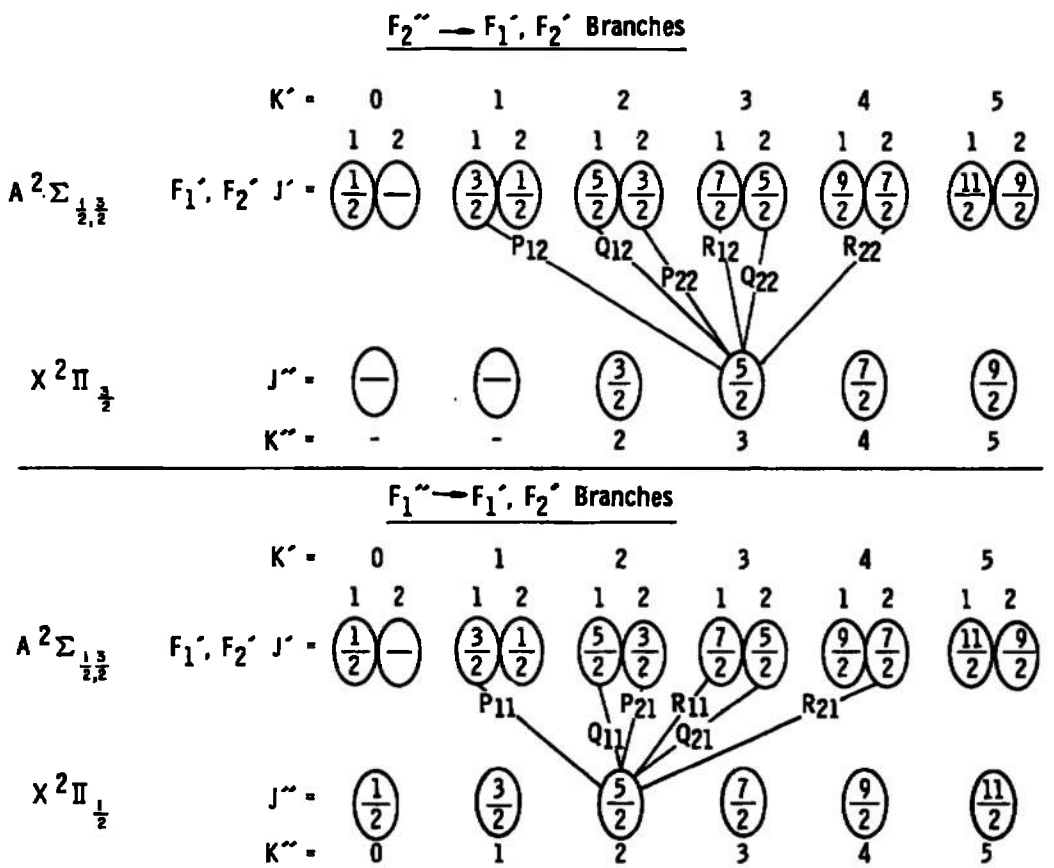

Fig. 4 Allowed Transitions for NO γ-Bands

The spectral lines for the v′ = 0 vibrational level of the A $^2\Sigma^+$ state to the v″ = 0 level of the X $^2\Pi$ state were calculated using Eq. (47) and the term formulas for each state given in Eqs. (40), (45), and (46) by means of a computer program written for the IBM 370-155 digital computer. The computer program is described in Appendix II. The calculated lines are shown in Fig. 5 in a way such that the individual lines can be identified. It will be observed that three distinct bandheads appear at 2269.7, 2268.6, and 2263.7 Å. Also, it can be seen that there is much overlapping of lines so that resolution of only a few individual lines is possible.

The computer program described in Appendix II also has the capability to simulate emission spectra that would be obtained from a real spectrometer. The program requires as inputs the oscillator strengths, or transition probabilities of the individual rotational lines of the bands

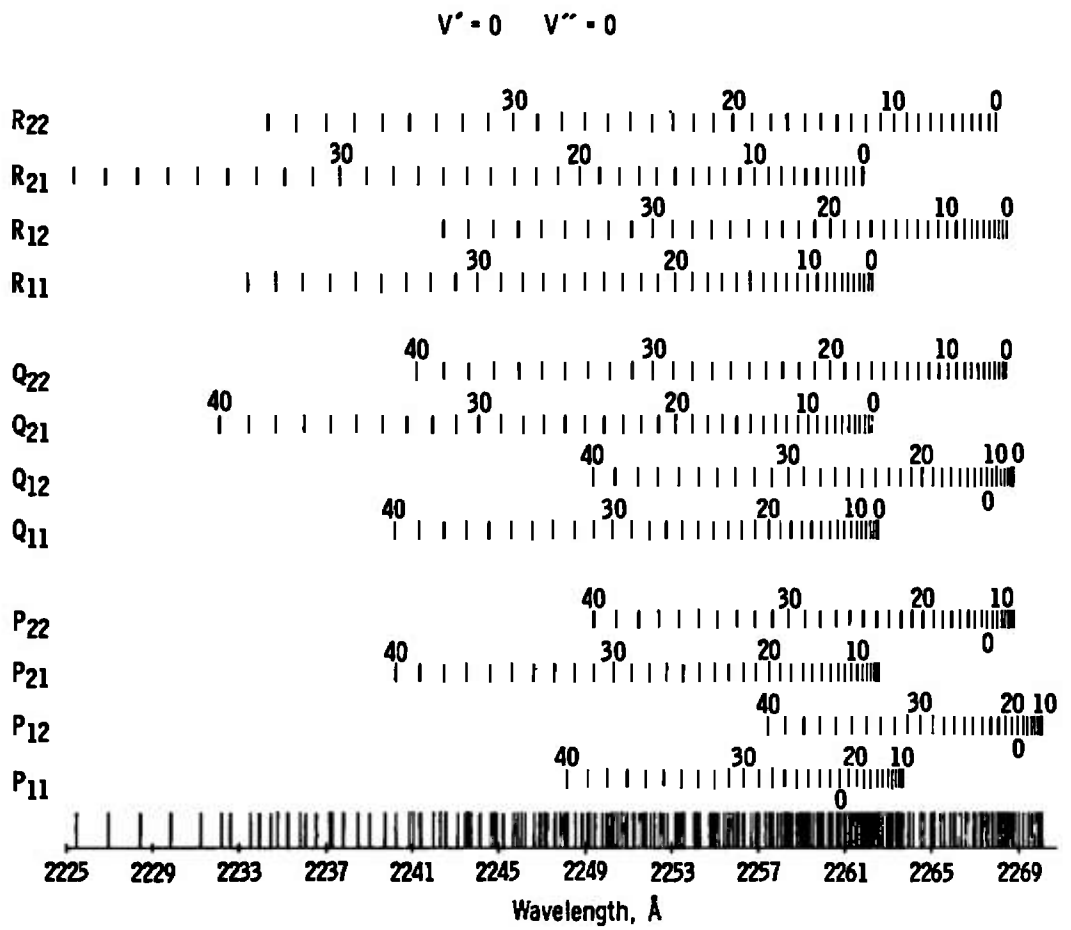

Fig. 5 Computer-Generated Band Structure for the NO (0,0) γ-Band

of interest, the temperature, and the instrument slit function. For the calculations presented in Appendix II, the oscillator strengths given in the next section for the NO molecule were used. The temperature was chosen as 775°K, which is characteristic of the source of radiation used (see Section IV). The instrument slit function was taken as triangular with a half-width of 0.03 Å, which corresponds to the slit width of the spectrometer used in the work reported here. The simulated spectrum of the (0,0) band of the γ-system appears in Fig. 6 in two plots, one having a slit function of zero half-width and one having the realistic, 0.03 Å half-width. The simulated spectrum is also characterized by the three distinct bandheads. Between these bandheads several distinct peaks are found which contain groupings of rotational lines. Some of these distinguishable peaks contain only two or three lines. Several peaks useful for measurements are designated in Fig. 6 as 1, 2, 3, etc., and the line components of the peaks are listed, together with their relative strength, in Table II. At wavelengths shorter than that of the P_{11} bandhead, the lines are badly overlapped and not useful for individual line measurements.

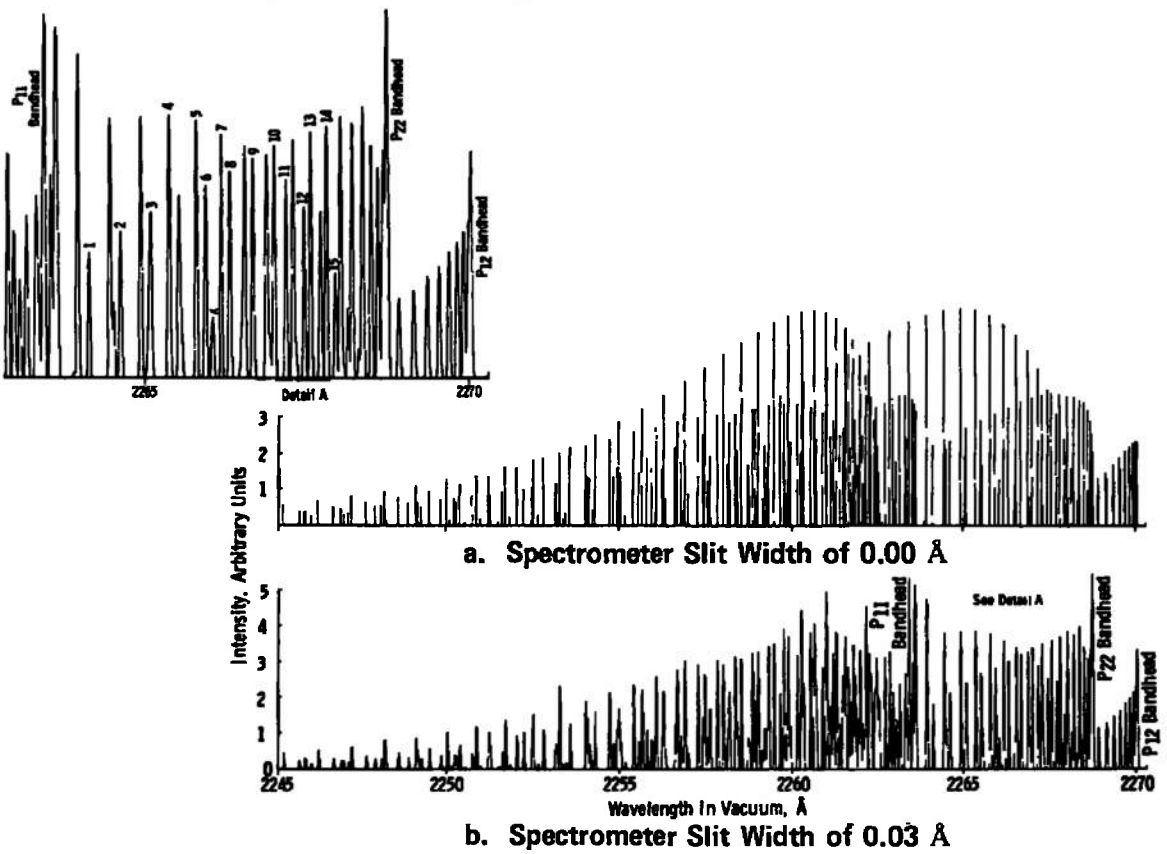

Fig. 6 Computer-Simulated Spectra for the NO (0,0) γ-Band at a Temperature of 775°K

TABLE II
LINE IDENTIFICATION AND DATA FOR SPECTRAL PEAKS USEFUL FOR NO CONCENTRATION MEASUREMENTS

Components	Wavelength (Å)	E(J'') (cm^{-1})	$\Sigma S_{J''}$	$[\lambda \Sigma S_{J''} \exp(-E_{J''}/203.7)]^{-1}$ x 10^{14}	C x 10^{15} cm^{-3}
1-P_{22}+Q_{12}(43/2)	2264.14	829.60	17.12+10.38=27.50	9.419	14.618
2-P_{22}+Q_{12}(41/2)	2264.64	755.80	16.18+10.26=26.44	6.786	10.532
3-P_{22}+Q_{12}(39/2)	2265.11	685.43	15.25+10.12=25.37	5.016	7.784
4-Q_{22}+R_{12}(23/2)	2265.40	288.75	14.95+3.38=18.33	0.991	1.538
5-Q_{22}+R_{12}(21/2)	2265.82	245.80	13.38+3.15=16.53	0.890	1.381
6-P_{22}+Q_{12}(35/2)	2265.96	554.96	13.43+9.76=23.19	2.872	4.457
x-R_{22}(11/2)	2266.07	82.53	2.44=2.44	2.712	4.209
7-Q_{22}+R_{12}(19/2)	2266.21	206.28	11.85+2.90=14.75	0.824	1.279
8-P_{22}+Q_{12}(33/2)	2266.35	494.87	12.54+9.54=22.08	2.245	3.484
9-P_{22}+Q_{12}(31/2)	2266.70	438.20	11.66+9.29=20.95	1.791	2.780
10-P_{22}+Q_{12}(29/2)	2267.03	384.95	10.81+9.00=19.81	1.453	2.255
11-Q_{22}+R_{12}(13/2)	2267.22	108.31	7.53+2.03=9.56	0.786	1.220
12-Q_{22}+R_{12}(13/2)	2267.50	82.53	6.18+1.70=7.88	0.839	1.302
13-P_{22}+Q_{12}(25/2)	2267.60	288.75	9.14+8.32=17.46	1.023	1.588
14-R_{22}+Q_{12}(23/2)	2267.85	245.80	8.34+7.92=16.26	0.864	1.341
15-Q_{22}+R_{12}(7/2)	2267.98	41.27	3.60+0.96=4.56	1.184	1.838

3.3 LINES CHOSEN FOR ABSORPTION MEASUREMENTS

The peaks given in Table II and shown in Fig. 6 which contain strong lines terminating in the same lower rotational state were considered to be the most useful for the absorption measurements. These are the groups containing only $Q_{22}(J'') + R_{12}(J'')$ or $P_{22}(J'') + Q_2(J'')$ lines; in other words, those containing only lines originating from a common lower rotational state. For example, the peak designated as 2 contains $P_{22}(41/2) + Q_{12}(41/2)$ lines and the peak designated as 4 contains only $Q_{22}(25/2) + R_{12}(25/2)$ lines. Only one peak was found which contains a single line, $R_{22}(15/2)$, which is marked X in Fig. 6. Other peaks are overlapped mainly with R_{22} branch lines and the computation of N_o would be difficult using these.

3.4 OSCILLATOR STRENGTHS FOR THE γ-SYSTEM

The oscillator strength ($f_{J'J''}$) as defined in Eq. (36) requires knowledge of $f_{v'v''}$ and $\delta_{J'J''}$. Perry-Thorne and Banfield (Ref. 16) have presented the latest results on determination of f_{00}, the

vibrational oscillator strength for the (0,0) band of the system. They give $f_{00} = 3.64 \pm 0.05 \times 10^{-4}$. Spindler, Isaacson, and Wentink (Ref. 17) have calculated values of $q_{v'v''}$, which are given in Table III, so that any $f_{v'v''}$ can be determined by use of Eq. (35).

TABLE III
FRANCK-CONDON FACTORS FOR THE γ-BANDS OF NO*

v′	v″					
	0	1	2	3	4	5
0	0.1615**	0.2586	0.2397	0.1625	0.0912	0.0470
	0.1524***	0.2476	0.2367	0.1688	0.0987	0.0514
1	0.3336	0.1046	0.0004	0.0675	0.1288	0.1329
	0.3277	0.1134	0.0000+	0.0566	0.1224	0.1319
2	0.2991	0.0162	0.1517	0.0738	0.0008	0.0310
	0.3029	0.0108	0.1444	0.0825	0.0028	0.0236
3	0.1490	0.1999	0.0443	0.0392	0.1105	0.0514
	0.1552	0.1900	0.0543	0.0287	0.1075	0.0583
4	0.0462	0.2443	0.0438	0.1228	0.0021	0.0541
	0.0496	0.2486	0.0329	0.1262	0.0054	0.0442
5	0.0094	0.1324	0.2217	0.0005	0.1026	0.0468
	0.0105	0.1405	0.2134	0.0031	0.0948	0.0545

* Taken from Spindler, Isaacson, and Wentink, Ref. 17

** $A\ ^2\Sigma - X\ ^2\Pi_{1/2}$

*** $A\ ^2\Sigma - X\ ^2\Pi_{3/2}$

Earls (Ref. 7) has published formulas for the normalized Hönl-London factors for $^2\Sigma - {}^2\Pi$ transitions, which apply to the γ-system of NO. The expressions are given in Table IV. As noted earlier, the measurement of absorption has to be on pairs of lines originating from the same J″, rather than individual lines. The pairs useful for absorption measurements consist of the P_{22} and Q_{12} lines, and the Q_{22} and R_{12} lines identified in Table II. Churchill, Hagstrom, and Landshoff

TABLE IV
HÖNL-LONDON FACTORS FOR $^2\Sigma \rightarrow {}^2\pi$ TRANSITIONS INTERMEDIATE BETWEEN HUND'S CASES (a) AND (b)*

$$R_{22} = \frac{(2J''+1)^2 + (2J''+1)[Y(Y-4) + (2J''+1)^2]^{-1/2}(4J''^2+4J''+1-2Y)}{8(J''+1)}$$

$$Q_{22} = \frac{(2J''+1)[(4J''^2+4J''-1) + \{Y(Y-4)+(2J''+1)^2\}^{-1/2}(8J''^3+12J''^2-2J''+1-2Y)]}{8J''(J''+1)}$$

$$P_{22} = \frac{(2J''+1)^2 + (2J''+1)[Y(Y-4)+(2J''+1)^2]^{-1/2}(4J''^2+4J''-7+2Y)}{8J''}$$

$$R_{12} = \frac{(2J''+1)^2 - (2J''+1)[Y(Y-4) + (2J''+1)^2]^{-1/2}(4J''^2+4J''-7+2Y)}{8(J''+1)}$$

$$Q_{12} = \frac{(2J''+1)[(4J''^2+4J''-1) - \{Y(Y-4) + (2J''+1)^2\}^{-1/2}(8J''^3+12J''^2-2J''-7+2Y)]}{8J''(J''+1)}$$

$$P_{12} = \frac{(2J''+1)^2 - (2J''+1)[Y(Y-4) + (2J''+1)^2]^{-1/2}(4J''^2+4J''+1-2Y)}{8J''}$$

$$R_{11} = \frac{(2J''+1)^2 - (2J''+1)[Y(Y-4) + (2J''+1)^2]^{-1/2}(4J''^2+4J''-7+2Y)}{8(J''+1)}$$

$$Q_{11} = \frac{(2J''+1)[(4J''^2-4J''-1) + \{Y(Y-4) + (2J''+1)^2\}^{-1/2}(8J''^3+12J''^2-2J''-7+2Y)]}{8J''(J''+1)}$$

$$P_{11} = \frac{(2J''+1)^2 + (2J''+1)[Y(Y-4) + (2J''+1)^2]^{-1/2}(4J''^2+4J''+1-2Y)}{8J''}$$

$$R_{21} = \frac{(2J''+1)^2 - (2J''+1)[Y(Y-4) + (2J''+1)^2]^{-1/2}(4J''^2+4J''+1-2Y)}{8(J''+1)}$$

$$Q_{21} = \frac{(2J''+1)[(4J''^2+4J''-1) - \{Y(Y-4) + (2J''+1)^2\}^{-1/2}(8J''^3+12J''^2-2J''+1-2Y)]}{8J''(J''+1)}$$

$$P_{21} = \frac{(2J''+1)^2 - (2J''+1)[Y(Y-4) + (2J''+1)^2]^{-1/2}(4J''^2+4J''-7+2Y)}{8J''}$$

where $Y = A'/B_v$

*Reference 7

(Ref. 14) have taken into account this overlapping of lines and have expressed the Hönl-London factors, where applicable, as the sum of the Hönl-London factor for each line as follows:

$$\Sigma\delta[Q_{22}(J'') + R_{12}(J'')] = \frac{2J''+1}{8J''}[(6J''-1) + U(4J''^2+4J''+1-2Y_v] \quad (48)$$

$$\Sigma\delta[P_{22}(J'') + Q_{12}(J'')] = \frac{2J''+1}{B(J''+1)}[(6J''+7) - U(4J''^2+4J''+1-2Y_v] \quad (49)$$

where J'' refers to the J-value in the $X\ ^2\Pi_{1/2,\,3/2}$ state for a given rotational transition. Here, U has the form

$$U = [Y_v^2 - 4Y_v + (2J''+1)^2]^{-1/2} \quad (50)$$

where $Y_V = A/B_V$ is the coupling factor. For the NO γ-system, A has a value of 124.2 cm^{-1}. The values of $\Sigma\delta_{J''}$ for these line pairs for the lines used in this study are also given in Table II.

3.5 MODIFICATION OF SPECTRAL LINE ABSORPTION THEORY FOR MULTIPLETS

Application of Eq. (34) for determining species concentrations requires summing over the two lines of the same wavelength. That is,

$$\sum_{J'}\left(\int_0^\infty k_\nu d\nu\right)_{J'J''} = \sqrt{\pi/4\ell n2}\ \sum_{J'}(\Delta\nu_D)_{J'J''}(k_{\nu_o})_{J'J''} \quad (51)$$

For a single line,

$$\int_0^\infty k_\nu d\nu = \frac{\pi e^2}{mc^2} N_{J''} f_{J'J''} \quad (52)$$

and for the pair of lines $(Q_{22} + R_{12})$,

$$\sum_{J'}\left(\int k_\nu d\nu\right)_{J'J''} = \frac{\pi e^2}{mc^2}\sum_{J'} N_{J''} f_{J'J''} = \frac{\pi e^2}{mc^2} N_{J''}\Sigma\delta[Q_{22}(J'') + R_{12}(J'')] \quad (53)$$

or, for the pair $P_{22} + Q_{12}$,

$$\sum_{J'}\left(\int k_\nu d\nu\right)_{J'J''} = \frac{\pi e^2}{mc^2} N_{J''}\Sigma\delta[P_{22}(J'') + Q_{12}(J'')]$$

Using Eqs. (45), (46), and (37) and grouping together quantities which explicitly depend on the rotational transitions result in an equation for the concentration:

$$N_o = \frac{mc^2/e^2}{\sqrt{4\pi \ell n 2}} \frac{2(2S+1)^2\, Q_v Q_r}{\exp\left[-G(v'')/\kappa T\right]} \frac{\lambda_{J'J''}}{\lambda_{v'v''}} \frac{\Delta\nu_D \sum_{J'} (k_{\nu_o})_{J'J''}}{f_{v'v''} (\sum_{J'} S_{J'J''}) \exp\left[-F(J'')/\kappa T\right]} \tag{54}$$

where the quantities $\lambda_{J'J''}$ and $(\Delta\nu_D)_{J'J''}$ are not included under the summations because they are the same for each line in the peak. The definition is made:

$$(\bar{k}_o)_{\nu_o} = \sum_{J'} (k_{\nu_o})_{J'J''} \tag{55}$$

where $(\bar{k}_o)_\nu$ is the measured absorption coefficient. The combination Hönl-London Factor $(\sum_{J'} S_{J'J''})$ is just the sum of the Hönl-London factors for the pair of lines $(Q_{22} + R_{12})$ or $(P_{22} + Q_{12})$, Eqs. (48) and (49).

3.6 FINAL WORKING EQUATIONS

The final step in developing a satisfactory working equation for predicting NO concentrations is the determination of the values of the parameters involved. The quantities in Eq. (54) are given as follows, using cgs units:

$$mc^2/e^2 = 3.555 \times 10^{12} \text{ gm cm}^2 \text{ sec}^{-2} \text{ esu}^{-2}$$

$$\sqrt{4\pi \ell n 2} = 2.953$$

$$2(2S+1)^2 = 8(S = 1/2)$$

$$Q_v/\exp\left[-G(v'')/\kappa T\right] \simeq 1.000 \qquad (T = 293°K)$$

$$Q_r = \sum_{J=0}^{\infty} (2J+1) \exp\left[-F(J)/\kappa T\right] \simeq \kappa T/B_o = 122.2 \qquad (T = 293°K)(\text{Ref. 10})$$

$$\lambda_{J'J''}/\lambda_{v'v''} \simeq 1$$

$$\Delta\nu_D = 2.228 \times 10^{-6} \lambda^{-1} \text{ cm}^{-1} \qquad (T = 293° K)$$

$$f_{oo} = 3.64 \times 10^{-4} \quad (\text{Ref. 16})$$

The absorption coefficient at the peak of the absorption line is determined from the relation

$$\bar{k}_{\nu_o} = \frac{1}{L} \ell n \left(\frac{I_m^o}{I_m} \right)_{\nu_o} \tag{56}$$

where L, the path length through the absorbing gas, is 45.72 cm (for the absorption tube used). The numerical equation for this measurement is thus obtained:

$$N_o = C \ell n \left(\frac{I_m^o}{I_m} \right)_{\nu_o} \tag{57}$$

where

$$C = \frac{7.22 \times 10^{12}}{L\lambda \exp[-E_{J''}/\kappa T] \begin{Bmatrix} S_{J''}(Q_{22} + R_{12}) \\ S_{J''}(P_{22} + Q_{12}) \end{Bmatrix}} = \frac{1.59 \times 10^{11}}{\lambda \exp[-E_{J''}/\kappa T] \begin{Bmatrix} S_{J''}(Q_{22} + R_{12}) \\ S_{J''}(P_{22} + Q_{12}) \end{Bmatrix}} \tag{58}$$

where λ is the wavelength at the measured peak in cm. Values of $S_{J''}(Q_{22})$, $S_{J''}(R_{12})$, $S_{J''}(P_{22})$, and $S_{J''}(Q_{12})$ are given in the tabulations for each line in Appendix II, and their sum is given for each of the peaks used for measurements in Table II. The numerical value of the J'' dependent part of Eq. (58) at a temperature of 293°K is also given in Table II.

SECTION IV
DESCRIPTION OF EXPERIMENT

4.1 APPARATUS

4.1.1 Ultraviolet Spectrometer

A 1-meter Jarrell-Ash grating spectrometer equipped with curved slits was used. The grating had 1180 lines/mm and was blazed at 7500 Å. A Hamamatsu-type R106 photomultiplier tube with S-19 spectral response was used as the detector. The external optics consisted of two fused silica lenses each with an f-number of 4.4. The lenses were placed, as shown in Fig. 7, such that parallel light from the source would pass through the absorbing gas and focus on the slit of

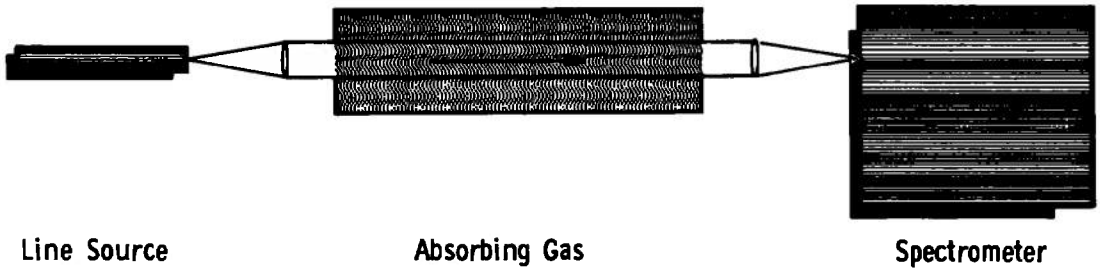

Fig. 7 Diagram of Experimental Apparatus

the spectrometer. A physical slit width of 10μ was used for the absorption measurements.

4.1.2 Source of NO Radiation

The source used was the discharge from a small, water-cooled capillary tube containing a mixture of A, N_2, and O_2 at a pressure of approximately 5mm Hg. A Fluke power supply, operated at 2800 v, was used to maintain a discharge which produced the NO radiation. The discharge was viewed along the axis of the tube. A diagram of the discharge tube is presented in Fig. 8.

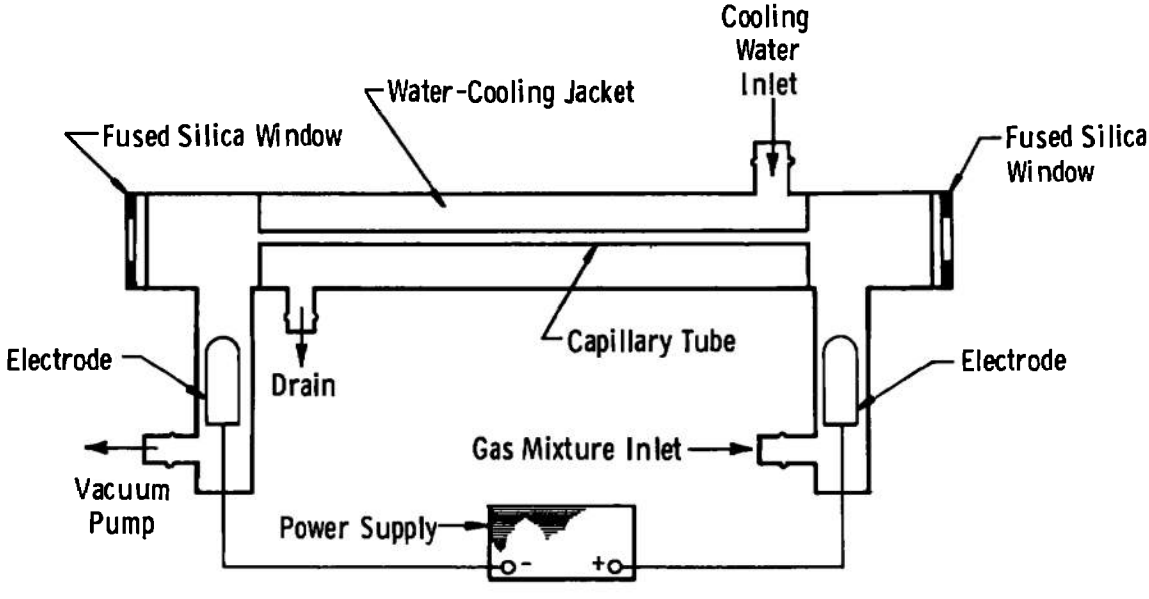

Fig. 8 Diagram of Discharge Tube Used to Produce NO γ-Band Radiation

4.1.3 Absorption Cell

The absorption cell was a stainless steel tube approximately 18 in. in length with an inner diameter of 1-7/8 in. Two 1/4-in.-thick fused silica windows were placed at each end. The cell had four stainless steel valves attached as shown in Fig. 9 to provide for evacuating the cell, bleeding in nitric oxide, bleeding in other gases, and isolating the pressure gage. The system was cleaned and dried before use with the NO. The NO was at room temperature which was 294 ± 1°K.

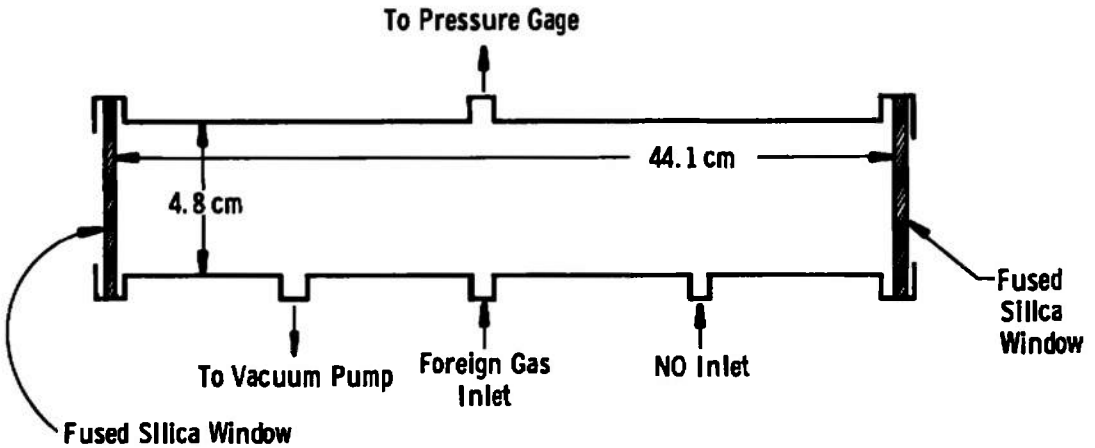

Fig. 9 Diagram of Absorption Cell Used to Contain Samples of NO at Known Pressure and Temperature

4.1.4 Data Recording System

The data recording system is shown in Fig. 10. A Fluke Model 412-B high-voltage power supply was used to provide excitation voltage for the photomultiplier tube. An operating voltage of 800 v was used because it provided the optimum signal-to-noise ratio. The photomultiplier tube signal was fed into a Philbrick Model P-2 operational amplifier having a gain of 100. The signal was recorded on a Mosely strip-chart recorder which graphically displayed the spectrum. Linearity of the system was checked using a standard potentiometer and found to be within 0.1 percent. The noise level encountered was found to give the largest instrument uncertainty (approximately ±2 percent) in the measurement.

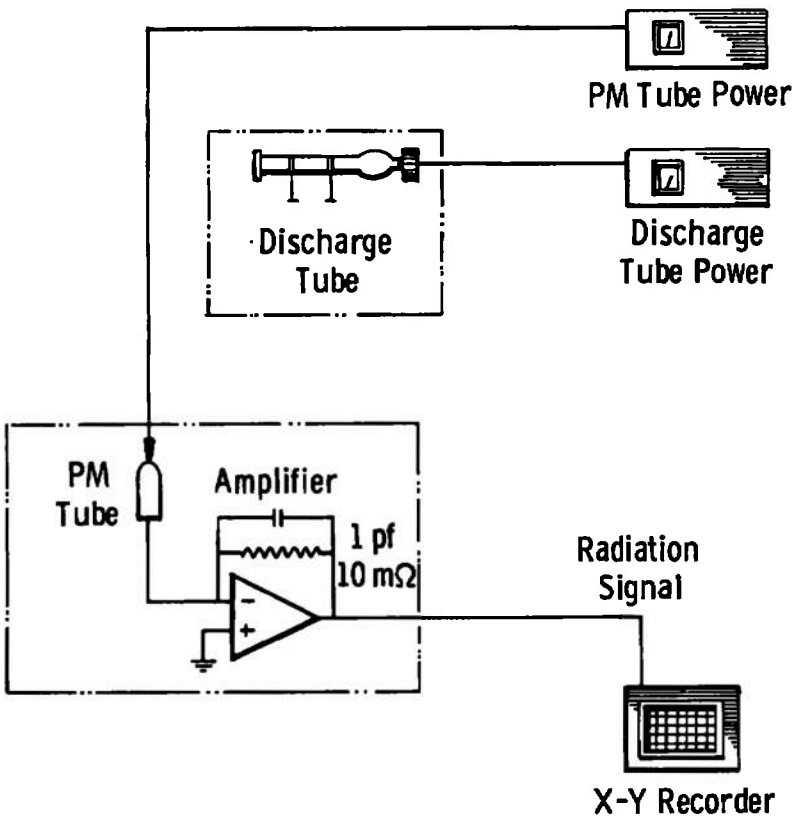

Fig. 10 Diagram of Data Recording System Used with Spectrometer

4.1.5 Gas Property Instruments

Knowledge of the pressure and temperature of the gas in the absorption cell was important so that number densities of NO molecules could be calculated to use for comparison with values obtained from the absorption measurements. A McLeod vacuum gage was used to measure the pressure. The limiting uncertainty of this gage is the readability, which for the range of pressures employed here, is about ±2.5 percent. The room temperature (assumed equal to the cell temperature) was measured using a mercury thermometer reading in degrees Centigrade. A maximum deviation of one degree from the

observed reading was assumed to be the maximum error. Thus, the maximum uncertainty in the density of the gas in the absorption tube is conservatively estimated to be ±3 percent.

4.2 PERFORMANCE OF NO RADIATION SOURCE

The discharge tube was operated using air, mixtures of NO with argon, and mixtures of N_2, O_2, and argon flowing through the tube at various pressures from about 100 microtorr to 5 torr. The most intense and stable radiation of the γ-bands was produced when a 12:3:1 mixture of $A:N_2:O_2$ was used at a pressure of 5 torr. The spectrum of the portion of the (0,0) band of interest to this study is shown in Fig. 11. This spectrum was obtained in second order of the 1-meter spectrometer using 10μ slits; under these conditions the resolution was approximately 0.05 Å with a measured equivalent instrument slit width of 0.037 Å. The simulated spectrum calculated for the estimated temperature of the source (373°K) and 0.03 Å instrument slit width is also shown for comparison. Obviously, the calculated line wavelengths and intensities do not exactly correspond to those of the discharge tube, but the comparison is close enough for line identification. The lines previously selected for the absorption measurement are indicated.

4.3 PROCEDURE FOR ABSORPTION MEASUREMENTS

The absorption tube was first evacuated to a pressure less than 10^{-3} torr and then a base line spectrum covering the wavelength range shown in Fig. 11 was taken. (The base line spectrum was the same with the absorption tube containing air at atmospheric pressure.) Then, the tube was filled with NO at a pressure of about 5 torr, which was found to give absorption of about 90 percent, and the spectral scan, over the wavelength range in Fig. 11, was made. The NO pressure was then reduced by opening the valve to the vacuum pump for a short time, and the spectrum was again obtained. This procedure was repeated over a range of pressures down to 0.018 torr. The pressure in the absorption tube was carefully measured using the McLeod gage for each condition. The tube was then evacuated completely, and a post base line spectra was obtained. In most runs no measurable drift in the intensity of radiation from the discharge tube could be detected.

Attempts were also made to test the effect of increased pressure from non-absorbing gases in the tube. However, it was found that only

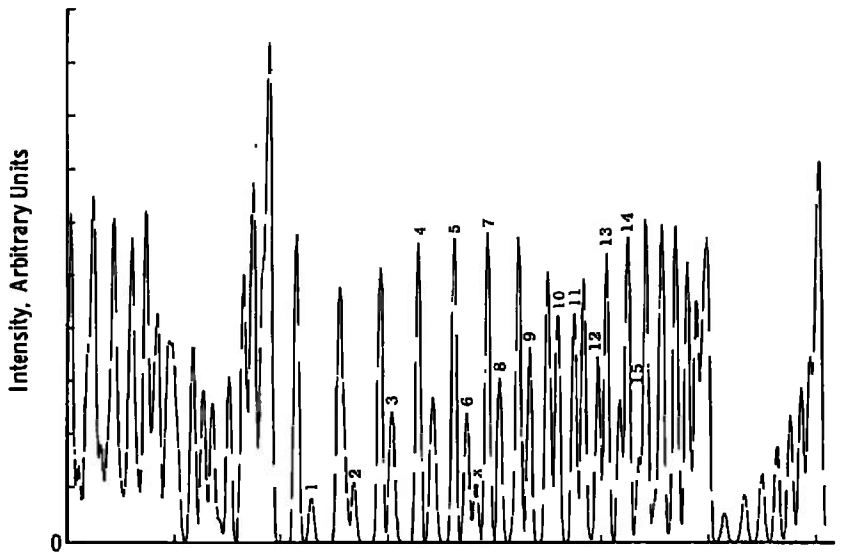

a. Computer-Simulated Spectra, Slit Width of 0.03 Å

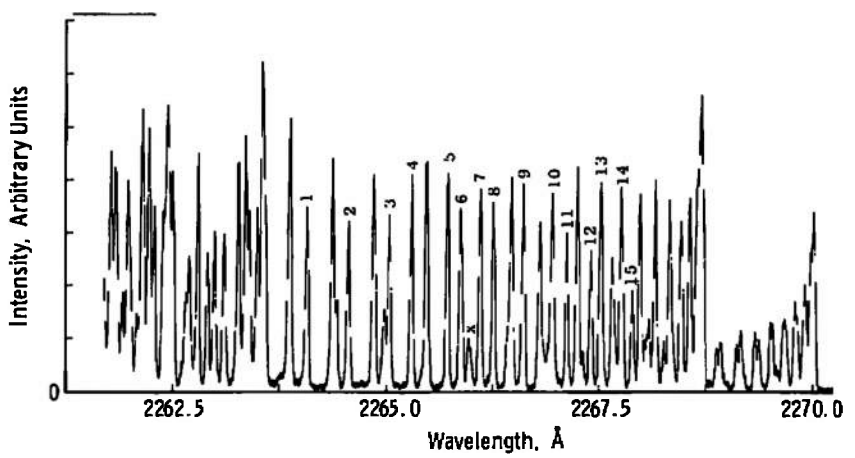

b. Spectrum from Source, Slit Width of 0.03 Å

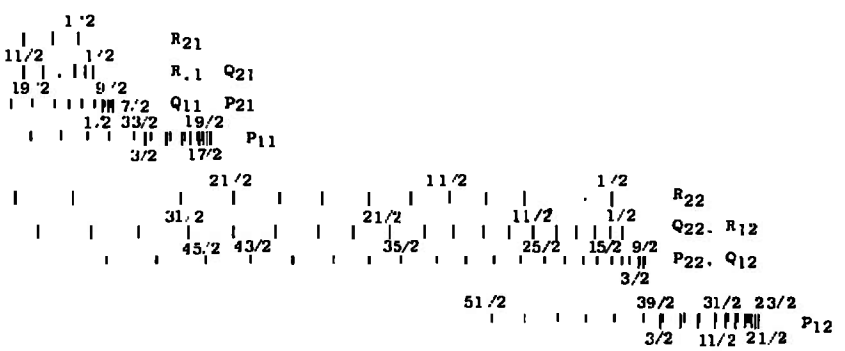

c. Rotational Line Location

Fig. 11 Portion of (0,0) NO γ-Band Used for Narrow Line Absorption Measurements

a few torr of air in the tube was sufficient to destroy the NO in a few seconds. Furthermore, with the system used, enough air was introduced when argon or helium was used as the diluent gas to produce the same effect.

SECTION V
RESULTS AND DISCUSSION

5.1 Results

A set of spectral scans of the NO (0,0) γ-band obtained at different pressures in the absorption cell is shown in Fig. 12. The lines used for the absorption measurements and calculations are indicated. The scans are shown in two sets which were run several days apart.

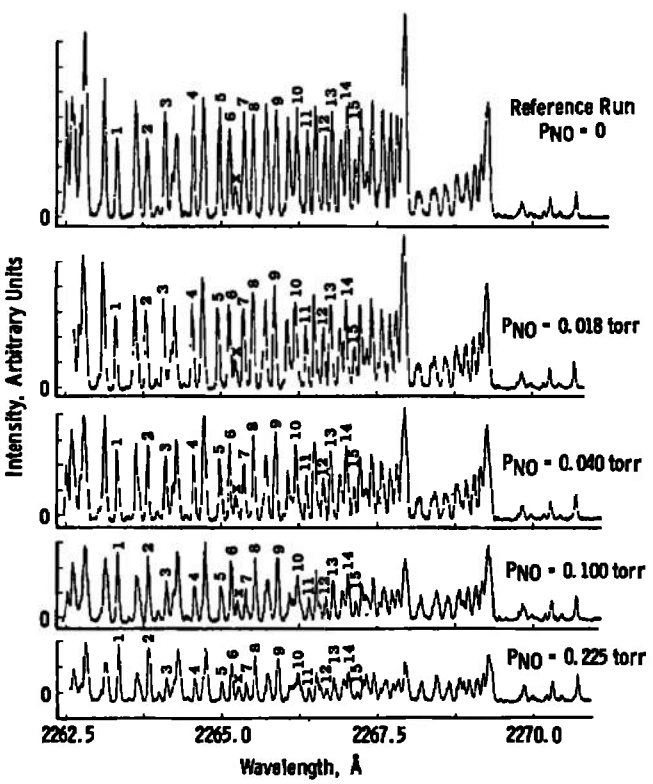

a. Run Number 1

Fig. 12 Experimental Data from Absorption Measurements of NO γ-Band Radiation Passing through a Low-Pressure Absorption Tube Containing NO

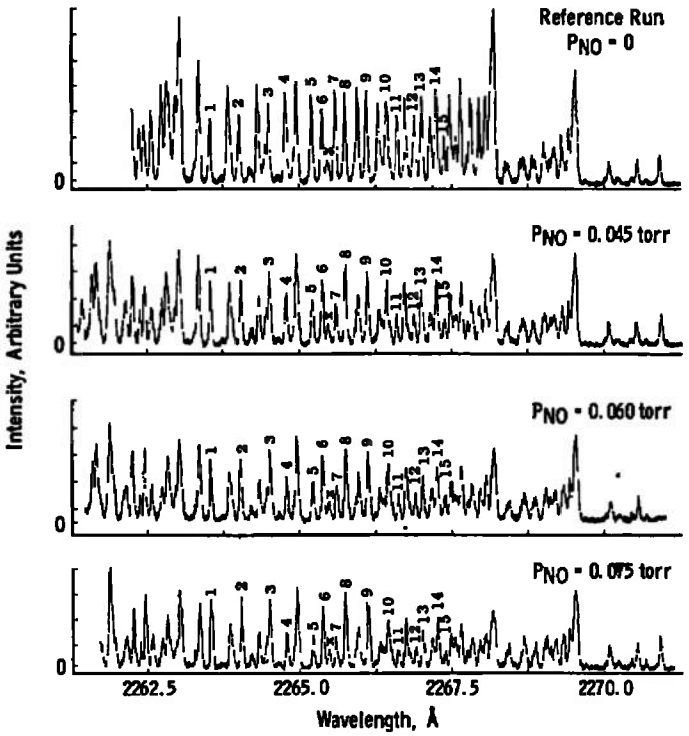

b. Run Number 2
Fig. 12 Concluded

The calculated density of NO as a function of the transmission $(I_m/I_m^o)_{\nu_o}$ using Eqs. (57) and (58) with the data from Table II is shown in Fig. 13 for several spectral lines. Also shown in Fig. 13 is the transmission at different densities calculated from the data in Fig. 12, and the transmission at line center for each of these data points obtained using the method of Appendix I. Agreement between theory and experiment is considered good (after the conversion from measured transmission to line center transmission is made) for those peaks containing $Q_{22} + R_{12}$ lines from a common J'' state when the transmission is greater than about 12 percent. For some reason (possibly overlap from adjacent lines), the $P_{22} + Q_{12}$ lines and the single R_{22} line give poor comparison to the theoretical curve. No consistent trend in the deviation from the theoretical for the $Q_{22} + R_{22}$ lines could be detected, and the deviations from the theoretical curve appear to be no larger than 20 percent.

Equations (57) and (58) may also be written in the form

$$\ln \frac{\ln I_m^o/I_m}{S_{J''}(Q_{22} + R_{12})} = \ln \frac{\lambda}{1.55 \times 10^{-11}} - \frac{E_{J''}}{\kappa T} \tag{59}$$

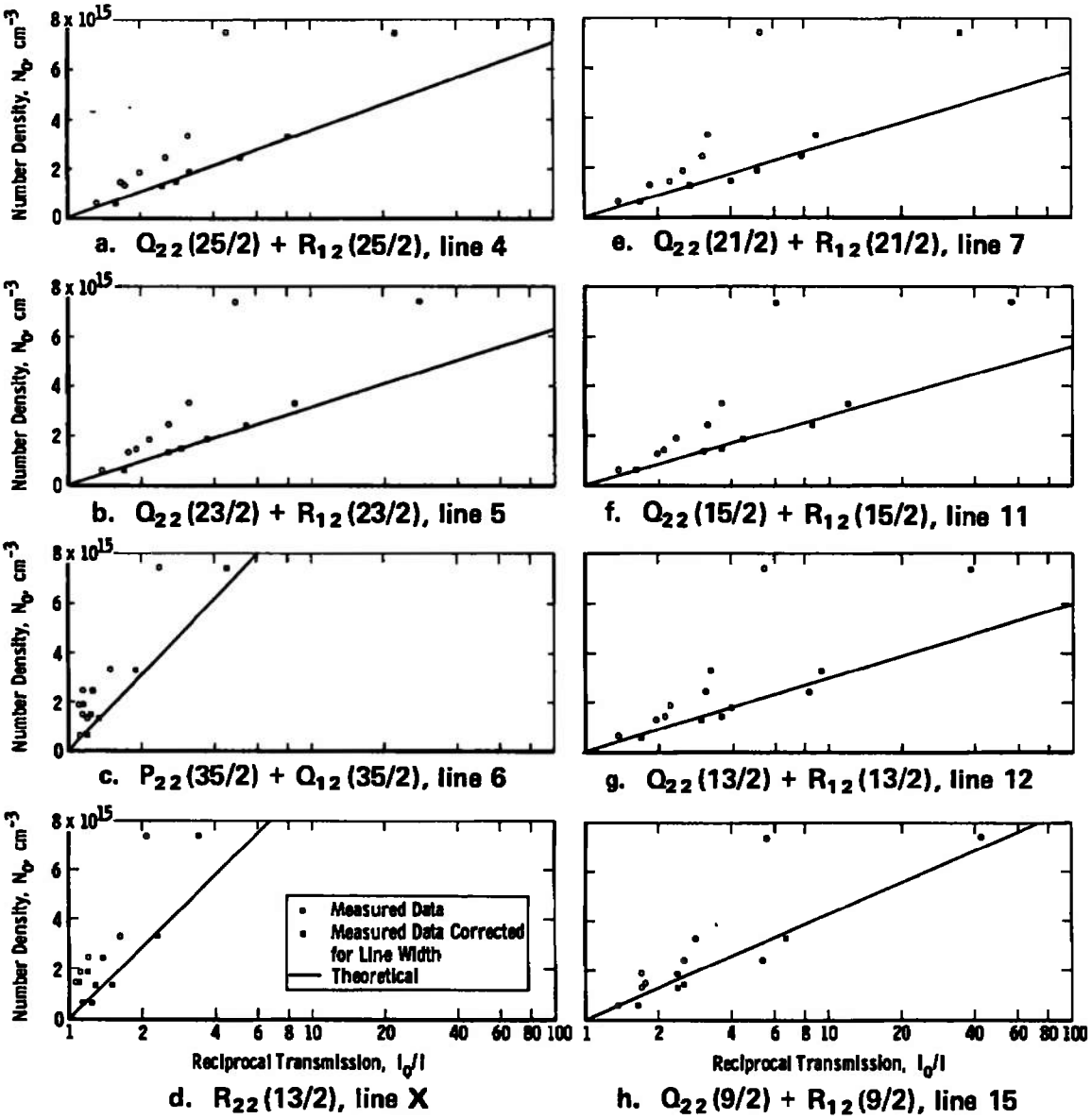

Fig. 13 Theoretical and Experimental Transmission of Several NO (0,0) γ-Band Lines through NO Gas at Various Pressures

where only the $Q_{22} + R_{12}$ lines have been included. When the left-hand side of the equation is plotted versus $E_{J''}$, a straight line should result having a slope of $1/\kappa T$, and thus the rotational temperature can be determined. Such a plot for the data of Fig. 13 and using the properties of Table II is given in Fig. 14. The least-squares straight line shown gives a temperature of 293°K, that is, room temperature. This result serves as a check on the method and also shows that the absorption data can be used for temperature measurement.

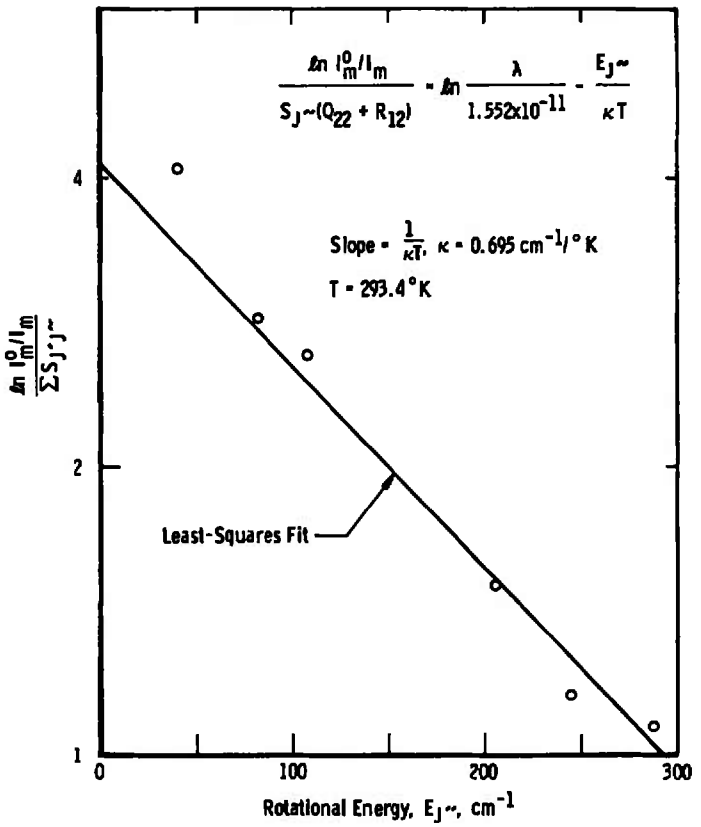

Fig. 14 Boltzmann Plot of Rotational Line Transmission for Determination of Rotational Temperature

5.2 Discussion of the Method

5.2.1 Validity of the Derived Working Equation

The work reported above serves to assemble the necessary analysis and molecular data for the use of measurement of the absorption coefficient of rotational lines in the γ-system of NO to determine concentration of the NO molecule. Furthermore, the experimental measurement serves to validate the accuracy of the derived working equations, Eqs. (57) and (58). This is gratifying for the following reasons. Derivation of an accurate expression such as Eq. (54) is tedious because of the bookkeeping necessary to keep track of the various statistical weights and partition junctions for rotational states of diatomic molecules. Moreover, the state of normalization of expressions for Hönl-London factors such as those expressed in Table IV (Ref. 7) is always suspect.

Expression of the Boltzmann population densities and line strengths must also be done in a systematic way. The approach taken by Tatum (Ref. 5) was strictly adhered to in this derivation, with apparent success.

5.2.2 Use of the Correction for Non-Narrow Line Source

The method for converting the measured transmission to line center transmission, when the source line width is about the same magnitude as the absorber line width, was of great use in this work. The ratio:

$$a = \frac{\Delta\lambda\,(\text{source})}{\Delta\lambda\,(\text{absorber})} \tag{60}$$

may be expressed as

$$a = \sqrt{\frac{T\,(\text{source})}{T\,(\text{absorber})}} \tag{61}$$

when Doppler broadening can be considered the principal broadening mechanism. In the experimental situation encountered in this report, the source temperature was estimated as 393°K while the temperature of the absorbing gas was room temperature (293°K). Then, a = 1.16, the value used in the correction. If the source temperature estimate is wrong by ±20°K, the correction curve shown in Appendix I will not change by an appreciable amount. The theoretical accuracy of the correction cannot be stated with any degree of confidence because of the complexity of the derivation (see Ref. 1). However, as shown by the data in Fig. 13, the correction works rather well.

As the temperature of the absorber gas increases to that typical of combustion gas streams, such as jet engine exhausts (one to three thousand degrees Kelvin), "a" becomes small, and the correction becomes less important. However, for use in the detection of NO in the atmosphere, the correction is necessary.

5.2.3 Non-Uniform Absorbing Media

The transmittance depends on the temperature and concentration along the absorbing path. If these are constant along the path, then Eq. (54) is directly applicable for determination of either concentration or temperature. If either temperature or concentration is variable along

the path, then additional knowledge is necessary to deduce profiles from measured transmittances. If the temperature profile is known from some other measurement, then the total number of absorbing molecules along the path can be determined by breaking the path up into any number of zones of constant temperature. If the absorbing gas stream is axisymetric, then the radial profile of both concentration and temperature can be determined by use of the Abel integral inversion technique as reported by Seiber (Ref. 3) and discussed previously. This method requires that several measurements be made through a plane of the axisymetric flow.

5.2.4 Range of Application

The concentration range is limited because of experimental constraints to values of I_o/I_m from about 1.05 to 10. This, in turn, limits the range in the product $k_o\ell$ from about 0.07 to 2.3. Since k_o varies as N_o, the range of N_o can be controlled somewhat by controlling the path length (ℓ). Some control over the range is also afforded by choice of the rotational line used, as illustrated in the curves in Fig. 13. For example, the $P_{22}(35/2) + Q_{12}(35/2)$ line can theoretically be used for values of N_o up to about 10^{16} cm^{-3} at room temperature, while the Q_{22}, R_{12} lines are only useful up to about 3×10^{15} cm^{-3}. The lower limit for all the useful lines in the (0,0) band of the NO γ-system is about 10^{14} cm^{-3}. If the temperature of the absorber is increased to 2000°K then the upper limit is reduced to about 10^{15} cm^{-3} for the P_{22}, Q_{22} lines but does not change appreciably for the Q_{22}, R_{12} lines.

The overall range of NO which can be measured using the absorption technique is mainly controlled by the value

$$f_{v'v''} \exp[-G(v'')/\kappa T] / \sum_{v''} \exp[-G(v'')/\kappa T] \tag{62}$$

in Eq. (54). For $v'' = 0$, the exponentials reduce to unity at room temperature so that, for the (0,0) band, this expression is just f_{oo}. However, for $v'' = 1$, $v' = 0$, the expression becomes

$$\frac{f_{01} \exp[-G(1)/\kappa T]}{\sum_{v} \exp[-G(v'')/\kappa T]} = \frac{q_{01}}{q_{oo}} f_{oo} \frac{\exp[-2828/(0.695)(293)]}{\exp[-950/(0.695)(293)]} \tag{63}$$

Values of the Franck-Condon factors are given in Ref. 17 and are listed in Table III. The expression has a value of $1.62 \times 10^{-4} f_{oo}$ and therefore, for the (0,1) band,

$$N_o = 4.45 \times 10^{16} \frac{\ell n\,(I_o/I_m)}{\bar{L}} \frac{1}{\lambda \exp[-E_{J''}/\kappa T] S_{J''}} \tag{64}$$

The measurable range of N_o for lines in the (0,1) band is thus from about 5×10^{17} to about 10^{19} cm^{-3}. Measurements in this range using the (0,1) band were made previously by Litton (Ref. 18).

5.2.5 Validity of Oscillator Strengths

After careful evaluation of the experiments reported in the literature, the value of f_{oo} selected for this study was that of Perry-Thorne and Banfield (Ref. 16), which was determined by the Hook interferometric technique. Hasson, Farmer, and Nichols (Ref. 19) have recently published new values obtained by a modification of this technique and have reviewed the values obtained by several investigators using several methods. Their concensus is that the value lies near 4.1×10^{-4}. The deviation of this value from that of Ref. 16 is ± 13 percent. The experiment carried out in this study would have detected consistent deviations greater than about 5 percent. Thus, it is concluded that the Perry-Thorne and Banfield value was not a bad choice, and that other published values may be somewhat high.

SECTION VI
CONCLUSIONS

The following conclusions can be reached from this study:

1. The theoretical approach to spectral line absorption, when details are carefully attended to, leads to accurate expression for the number density of NO in terms of the measured line transmission, molecular properties, and the gas temperature.
2. The oscillator strength reported in the literature by Perry-Thorne and Banfield (Ref. 16) appears to be correct.
3. Application of the correction of measured transmission to transmission at line center, using the method of Mitchel and Zemansky (Ref. 1), is necessary when the temperature of the absorbing gas is not much greater than that of the source, and appears adequate for absorption values not exceeding about 50 percent.

4. The method, as applied here, using the (0,0) γ-band leads to determinations of NO number density with an uncertainty not exceeding 20 percent for values of N_o between about 10^{14} and 3×10^{15} cm^{-3}, at path lengths of about 50 cm. The range can be adjusted somewhat by choice of spectral line used or the path length. For larger densities, the (0,1), (0,2), etc., bands may also be used.

REFERENCES

1. Mitchel, A. C. G. and Zemansky, M. W. Resonance Radiation and Excited Atoms. The McMillan Co., New York, 1934.
2. Davis, M. G., McGregor, W. K., and Mason, A. A. "Determination of the Excitation Reaction of the OH Radical in H_2-O_2 Combustion." AEDC-TR-69-95 (AD695471), Oct. 1969.
3. Seiber, B. L. "Narrow Line OH Absorption Diagnostics of Cylindrically Symmetric Combustion Gas Streams." AEDC-TR-
4. Thorson, W. R. and Badger, R. M. "On the Pressure Broadening in the Gamma Bands of Nitric Oxide." Journal of Chemical Physics, Vol. 27, p. 609, September 1957.
5. Tatum, J. B. "The Interpretation of Intensities in Diatomic Molecular Spectra." The Astrophysical Journal, supplement No. 124, p. 21, March 1967.
6. Schadee, A. "The Relation between the Electronic Oscillator Strength and the Wavelength for Diatomic Molecules." Journal of Quantitative Spectroscopy and Radiative Transfer, Vol. 7, p. 169, 1967.
7. Earls, L. T. "Rotational Strength Factors for $^2\Sigma \rightarrow {}^2\Pi$ Transitions." Physical Review, Vol. 48, p. 423, 1935.
8. Kovacs, L. Rotational Structure in the Spectra of Diatomic Molecules, Adam Hilger Ltd, London, 1969.
9. Gero, L. and Schmid, R. "Dissociation Energy of the NO Molecule." Proceedings of the Physical Society, Vol. 60, p. 533, 1947.

10. Herzberg, G. Spectra of Diatomic Molecules. van Nostrand Co., Inc., New York, 1950.

11. Deezsi, I. "A Recent Rotational Analysis of the γ-Bands of the NO Molecule." Acta Physica, Vol. 9, p. 125, 1957.

12. Gero, L., Schmid, R., and von Szily, F. K. "Rotations Analyse der E-Banden des NO-Molekuls." Physica, Band 11 p. 144, Maart, 1944.

13. Gillette, R. H. and Eyster, E. H. "The Fundamental Rotation-Vibration Band of Nitric Oxide." Physical Review, Vol. 57, p. 1113, December 1939.

14. Churchill, D. R., Hagstrom, S. A., and Landshoff, R. K. M. "The Spectral Coefficient of Heated Air." The Journal of Quantitative Spectroscopy and Radiative Transfer, Vol. 4, p. 291, 1964.

15. Barrow, R. F. and Miescher, E. "Fine Structure Analysis of NO Absorption Bands in the Schumann Region." Proceedings of the Physical Society, Vol. A70, p. 219, 1957.

16. Perry-Thorne, A. and Banfield, F. P. "Absolute Oscillator Strength of Nitric Oxide by the Hook Method." Journal of Physics B, Atomic and Molecular Physics, Vol. 3, p. 1011, 1970.

17. Spindler, R. J., Isaacson, L., and Wentink, T. "Franck-Condon Factors and r-Centroids for the Gamma System of NO." Journal of Quantitative Spectroscopy and Radiation Transfer, Vol. 10, p. 621, 1970.

18. Litton, C. D. "Development of a Technique for Measuring Nitric Oxide Concentration." M. S. Thesis, The University of Tennessee, June 1971.

19. Hasson, V., Farmer, A. J. D., Nichols, R. W., and Anketell, J. "Oscillator Strength of the (0,0) Band of NO - $\gamma(A\ ^2\Sigma - X\ ^2\Pi)$ System." The Journal of Physics B, Atomic and Molecular Physics, Vol. 5, p. 1248, June 1972.

APPENDIXES

I. DESCRIPTION OF METHOD FOR CONVERSION OF MEASURED LINE TRANSMISSION TO LINE CENTER TRANSMISSION FOR NON-NARROW LINE SOURCES

II. DESCRIPTION OF COMPUTER SIMULATION AND BAND SPECTRA

APPENDIX I
DESCRIPTION OF METHOD FOR CONVERSION OF MEASURED LINE TRANSMISSION TO LINE CENTER TRANSMISSION FOR NON-NARROW LINE SOURCES

The accurate measurement of the absorption coefficient at line center (k_{ν_o}) is the key to the "narrow line absorption method." The ideal case is one in which the line source has a width that is much narrower than the absorption line. In the practical case, this condition is rarely met, but, fortunately, a correction can be made to the measured transmission that adequately compensates for the experimental condition. The basic requirements for the correction are given by Mitchell and Zemansky (Ref. 1).

The general expression for the measured transmission (t_m) is

$$t_m = \frac{\int I_\nu \, d\nu}{\int I_\nu^o \, d\nu} \tag{I-1}$$

where I_ν^o is the incident spectral intensity and I_ν is the transmitted spectral intensity at a frequency (ν), I_ν is related to I_ν^o by

$$I_\nu = I_\nu^o \exp(-k_\nu \ell) \tag{I-2}$$

If the absorption line is subject only to Doppler broadening, then

$$k_\nu = k_{\nu_o} \exp\left\{-\left[2\frac{(\nu - \nu_o)}{\Delta\nu_D}\sqrt{\ell n\, 2}\right]^2\right\} = k_{\nu_o} \exp(-W^2) \tag{I-3}$$

where k_{ν_o} is the absorption coefficient at the line center frequency (ν_o), $\Delta\nu_D$ is the width of the Doppler profile at half intensity, and W has the obvious definition. Thus

$$I_\nu = I_\nu^o \exp[-k_{\nu_o} \ell \exp(-W^2)] \tag{I-4}$$

Now, let

$$a = \frac{\text{emitter Doppler width}}{\text{absorber Doppler width}}$$

then

$$I_\nu^o = I_{\nu_o}^o \exp[-(W/a)^2] \tag{I-5}$$

Substituting Eqs. (I-4) and (I-5) into Eq. (I-1) gives the transmission:

$$t_m = \frac{\int_0^\infty \exp\left[-(W/a)^2\right] \exp\left\{\left[-k_{\nu_o} \ell\right] \exp\left[-W^2\right]\right\} dW}{\int_0^\infty \exp\left[-(W/a)^2\right] dW} \tag{I-6}$$

As shown in Ref. 1, this expression can be expanded in a series as follows:

$$t_m = 1 - \frac{k_{\nu_o} \ell}{\sqrt{1 + a^2}} + \frac{(k_{\nu_o} \ell)^2}{2! \sqrt{1 + 2a^2}} + \cdots + (-1)^{n-1} \frac{(k_{\nu_o} \ell)^n}{n! \sqrt{1 + na^2}} + \cdots \tag{I-7}$$

Equation (I-6), or (I-7), expresses the actual, measured value of the transmission (t_m) in terms of the true value of the transmission at the line center ($k_{\nu_o} \ell = \ell n(I_{\nu_o} / I^o_{\nu_o}) = \ell n\, t_{\nu_o}$) through the parameter (a). For Doppler broadening,

$$\Delta\nu_D = 2\nu_o \sqrt{\frac{2\kappa T \ell n 2}{Mc^2}} \tag{I-8}$$

where κ is Boltzmann's constant, M is the molecular weight, c is the velocity of light, and T is the temperature, so that

$$a = \sqrt{\frac{T(\text{source})}{T(\text{absorber})}} \tag{I-9}$$

Equation (I-6) can be evaluated numerically to give t_m as a function of ν_o with "a" as a parameter.

In Fig. (I-1) is plotted t_m^{-1} versus $t_{\nu_o}^{-1}$ for several values of "a" ranging from 0 to 1.5. The particular value of a = 1.16 applies to the condition of a 110°C source temperature being transmitted through a room temperature (20°C) absorber. For example, at this condition, a measured value of $t_m^{-1} = 2$ when corrected for a = 1.16 becomes $t_{\nu_o} = 3.15$; that is, the measured 50-percent transmission would be 32-percent transmission if a = 0, the condition of a very narrow emission line.

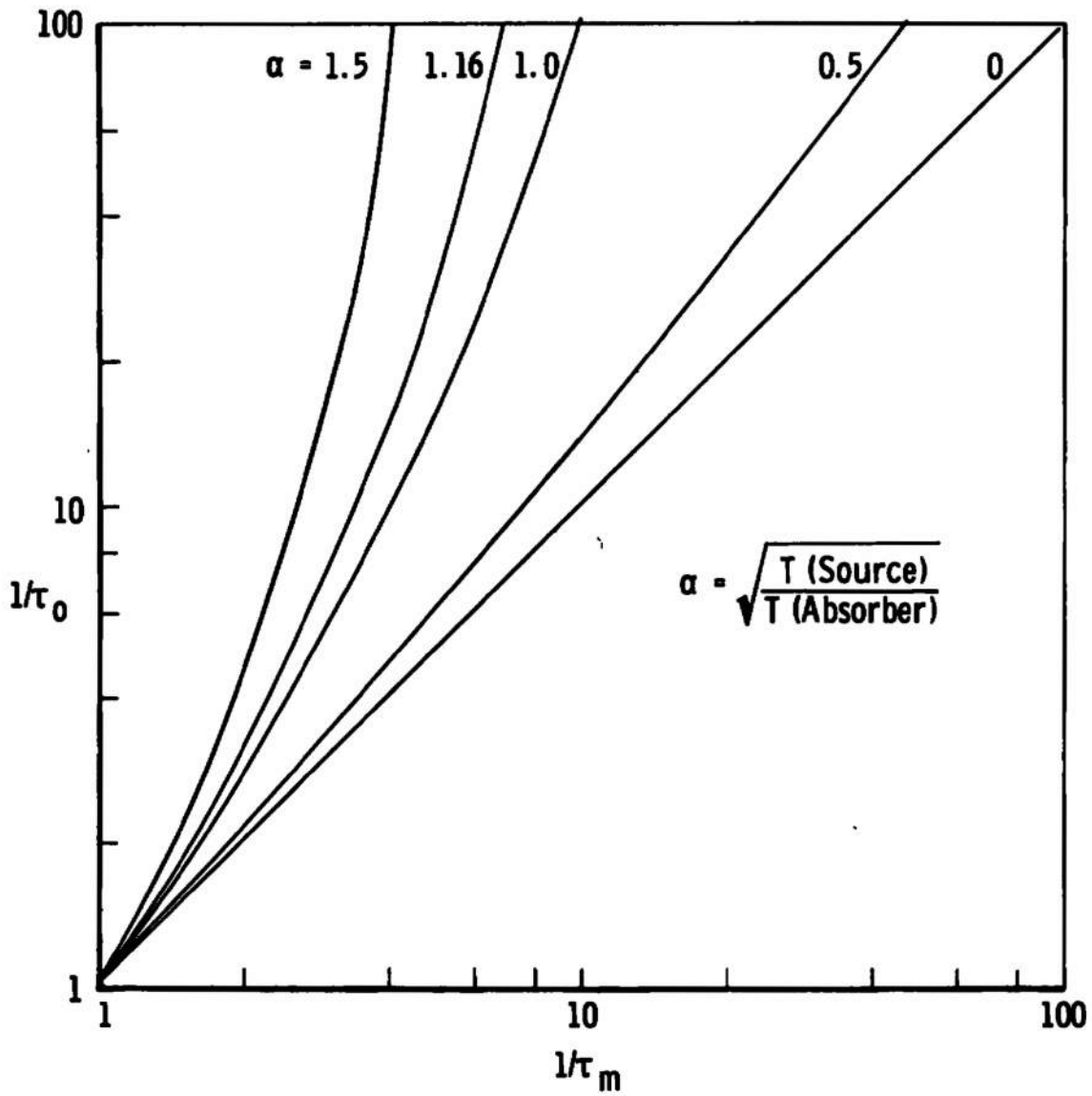

Fig. I-1 Conversion of Measured Transmission at Line Center for Doppler Broadened Lines (Ref. 1)

APPENDIX II
DESCRIPTION OF COMPUTER SIMULATION AND BAND SPECTRA

A computer program and plotting procedure for computing and simulating the rotational structure of vibrational bands in electronic transitions of diatomic molecules is described in this appendix. The program proceeds to compute and print out the energy levels in cm^{-1} for the upper and lower states selected for the transition, using the standard equations (Ref. 10):

$$\underline{\text{Upper}} \quad \mathcal{T}' = \mathcal{T}_e' + G'(v') + F_n'(J') \tag{II-1}$$

$$\underline{\text{Lower}} \quad \mathcal{T}'' = \mathcal{T}_e'' + G''(v'') + F_n''(J'') \tag{II-2}$$

where

$\mathcal{T}$ – total energy of the state

$\mathcal{T}_e$ – electronic state energy at v = 0, J = 0

G(v) – vibrational energy of the v = 0, 1, 2, 3 · · · vibrational state

$F_n(J)$ – rotational energy of the J = 0, 1, 2, · · · rotational state for multiplet states, n = 1, 2, 3, · · · so that $\mathcal{T}$ has a different value for each multiplet

The standard equation is used throughout for the vibrational energy:

$$G(v) = \omega_e(v + 1/2) - \omega_e x_e(v + 1/2)^2 + \omega_e y_e(v + 1/2)^2, \; v = 0, 1, 2 \cdots \tag{II-3}$$

The quantities ω_e, $\omega_e x_e$, and $\omega_e y_e$ are vibrational constants of the molecule which may generally be found in Herzberg (Ref. 10) or in the published literature. In special cases, the constants may be different for the different components of a multiplet.

The expression (F_n) for the rotational energy term is usually different for each molecule and is considered as an input to the program. All Σ states belong to Hund's coupling case "b" (Ref. 10), and for $^2\Sigma$ states (the upper state for the NO γ-band system is a $^2\Sigma$ state), the equations are

$$F_1(J') = B_v(J' + 1/2)(J' - 1/2) + 1/2\Gamma(J' - 1/2) - D_v(J' + 1/2)^2(J' - 1/2)^2$$
$$J' = 1/2, 3/2, 5/2, \cdots \tag{II-4a}$$

$$F_2(J') = B_v(J'+1/2)(J'+3/2) - 1/2\Gamma(J'+3/2) - D_v(J'+1/2)^2(J'+3/2)^2 \quad \text{(II-4b)}$$
$$J' = 1/2, 3/2, 5/2, \cdots$$

The rotational constants B_V and D_V depend on v and are given by

$$B_v = B_e - \alpha_e(v+1/2) \quad \text{(II-5)}$$

$$D_v = D_e + \beta_e(v+1/2) \quad \text{(II-6)}$$

with B_e, α_e, D_e, and β_e constant. The constant Γ is known as the spin splitting constant and is usually very small for Σ states. The lower rotational state of NO is a $^2\Pi$ state intermediate between Hund's cases "a" and "b" and for such a case the Hill and van Fleck formula was derived (Ref. 10). It is expressed as follows:

$$F_1(J'') = B_v[(J''+1/2)^2 - 1 - u] - D_vJ''^4 \quad \text{(II-7a)}$$

$$F_2(J'') = B_v[(J''+1/2)^2 - 1 + u] - D_v(J''+1)^4 \quad \text{(II-7b)}$$

where B_V and D_V are expressed as in Eqs. (II-5) and (II-6) and u is given by

$$u = [(J''+1/2)^2 - Y_v(1 - Y_v/4)]^{1/2} \quad \text{(II-8)} \quad \text{(II-8)}$$

with $Y_V = A/B_V$, A being the coupling constant.

The constants for NO used in these calculations were the most accurate available; for the $X\ ^2\Pi$ state, the values of Gillette and Eyster (Ref. 13) were used, and for the $A\ ^2\Sigma$ state, those obtained by Barrow and Miescher (Ref. 15) were used. The term values are given for J values out to 81/2 for the v = 0 and v = 1 vibrational states in Table II-1.

The spectral line computations are made in the program from the equation:

$$\nu = \frac{1}{\lambda} = \mathcal{T}' - \mathcal{T}'' \text{ cm}^{-1}$$
$$= (\mathcal{T}_e' - \mathcal{T}_e'') + [G(v') - G(v'')] + [F_n(J') - F_n(J'')] \quad \text{(II-9)}$$
$$\Delta v = 0, \pm1, \pm2, \cdots$$

$$\Delta J = \begin{cases} +1 & \text{R branches} \\ 0 & \text{Q branches} \\ -1 & \text{P branches} \end{cases}$$

Each kind of transition, $^2\Sigma \rightarrow {}^2\Pi$, $^3\Sigma \rightarrow {}^3\Pi$, $^1\Delta \rightarrow {}^1\Sigma$, etc., has its own peruliarities (Q formed P branches, R formed Q branches, etc.) which are described adequately by Herzberg (Ref. 10). Suffice it to say here that the computer programming problem in computing these spectral line wavelengths is mainly one of tedious bookkeeping. For the NO molecule, all 12 possible doublet-to-doublet transitions are present, and the details of the structure are explained in the text of this report. The computed spectra (ν and λ) are given in Table II-2 for all the branches of the (0,0) band.

Two methods of plotting the spectra are available. First, the lines of the different branches of a single band may be separated and then combined as shown in Fig. 5 of the text. This plot is similar to what would be observed on a photographic plate from a spectrograph and permits identification of the individual lines. It is of especial value in determining which lines overlap in a spectrum of given resolving power.

In the second method of plotting, an attempt is made to simulate the spectrum that would be produced by a monochrometer. For this purpose, it is also necessary to compute the intensities of the lines. Most sources produce spectra that exhibit near-Boltzmann-like distributions in rotational line distribution with some less-Boltzmann-like vibrational distributions. For purposes of comparison of computed spectra to real spectra, the assumption of a Boltzmann distribution was made. Then, the emission coefficient ($\epsilon_{J'J''}$) of the rotational lines within a band are given by

$$\epsilon_{J'J''} = \frac{hc}{\lambda_{J'J''}} A_{n'n''} q_{v'v''} \frac{\delta_{J'J''}}{(2J'+1)g_{n'}} \qquad \text{(II-10)}$$

where

h = Plank's constant, erg sec

c = velocity of light, cm/sec

$\lambda_{J'J''}$ = wavelength of the spectral line produced by the $J' - J''$ transition, cm

$q_{v'v''}$ = vibrational overlap integral, or Franck-Condon factor (Ref. 10)

$\delta_{J'J''}$ = rotational strength, or Hönl-London factor for the rotational transition

$2S' + 1$ = statistical weight of the rotational level

$g_{n'}$ = statistical weight of the electronic level; equal to $(2S + 1)$ for Σ states or $2(2S + 1)$ for other states

$N(n', v', J')$ = number of molecules occupying the J' rotational state in the v' vibrational level of the n' electronic level

For the Boltzmann distribution, the distribution of vibrational and rotational states within the electronic level is given by

$$N(v',J') = N_o \frac{\exp[-G(v')/\kappa T]}{\sum_{v'} \exp[-G(v')/\kappa T]} \times \frac{g_{J'} \exp[(-F_n J')/\kappa T]}{\sum_{J'} g_{J'} \exp[(-F_n G v')/\kappa T]} \qquad \text{(II-11)}$$

where:

$$\begin{aligned} N_o &= \text{total number of molecules} \\ \kappa &= \text{Boltzmann's constant, } 0.6952 \text{ cm}^{-1}/^\circ\text{K} \\ T &= \text{Temperature} \\ g_{J'} &= \text{statistical weight of the rotational state; usually} \\ g_{J'} &= (2S+1)(2J''+1), \ \Sigma \text{ states} \\ &\quad 2(2S+1)(2J'+1), \text{ other states} \end{aligned} \qquad \text{(II-12)}$$

(See Ref. 5 for exceptions to this expression.) The computation of the intensity of each line proceeds from Eqs. (II-10) and (II-11). The values of $A_{n'n''}$ and $q_{v'v''}$ are found in the literature for most bands. If the interest is only in the rotational distribution with a band, then the product of all the terms not explicitly dependent on J' may be set to unity. This is done in the present report. Or, the entire equation may be utilized if all the terms are known.

The quantity $\delta_{J'J''}$ must be given special attention, since, for other than singlet transitions, it may become quite involved. Expressions for $\delta_{J'J''}$ like F(J) are usually different for each case computed and depend on the electronic momentum states and the degree of coupling of orbital, spin, and rotational angular momentum as expressed by Hund's coupling cases. For the $^2\Sigma \rightarrow {}^2\Pi$ transition with the $^2\Pi$ state intermediate between Hund's cases "a" and "b" (the case for NO γ-bands), the formulas of Table IV are used. In the computer program the expression for $_{J'J''}$ is input for each spectra to be calculated.

The simulation of the monochrometer as usually recorded on a strip chart recorder is accomplished by numerical integration of the components of each line as determined by the wavelength, the line strength, the line width, and the monochrometer bandpass. The line width consideration will not be a part of this Appendix because the line broadening (natural, pressure, Doppler, Stark) encountered in this study are much smaller than the bandpass of the instrument used. However, the computer program is capable of handling these phenomena. The instrument band pass is taken here as a triangular function:

$$\int \epsilon_\lambda d\lambda \epsilon = \epsilon_o \begin{cases} \dfrac{\Delta\lambda - (\lambda_o - \lambda)}{\Delta\lambda}, \lambda < \lambda_o; 0, \lambda < \lambda_o - \Delta\lambda \\ \dfrac{\Delta\lambda - (\lambda - \lambda_o)}{\Delta\lambda}, \lambda > \lambda_o; 0, \lambda > \lambda_o + \Delta\lambda \end{cases} \quad \text{(II-13)}$$

where ϵ_o is the emission coefficient as computed in Eq. (II-10), λ_o is the wavelength at the center of the line, and $\Delta\lambda$ is the half-width of the triangular bandpass. The equivalent half-width in wavelength units is given by the product of the reciprocal dispersion (Å/mm) of the instrument and the actual instrument slit width in mm (assuming entrance and exit slit widths are equal as in the case for all work reported here). The computer is then given a temperature, $\Delta\lambda$, the molecule constants, and a wavelength plotting scale (Å per inch of recording paper) which is the same as the experimental scale. Simulated spectra for the (0,0) band of the NO γ-system then appear as in Fig. 6. If the overlap of lines within an apparent peak is suspected, then $\Delta\lambda$ may be set equal to zero, and the spectrum as plotted in Fig. 6 results.

This computer program is of great utility in studies of the nature of this report, and line identification from experimental data is almost impossible without it. The program is written for the IBM-370/155 computer with a Cal-Comp plotter.

TABLE II-1
TERM VALUES FOR THE $A^2\Sigma$ AND THE $X^2\Pi$ STATES OF NO IN WAVE NUMBERS

$v'' = 0$, $X\ ^2\Pi$ State

	$F_1(J'')$	$F_2(J'')$
J= 0.5	-9.503528E 02	-1.070851E 03
J= 1.5	-9.553684E 02	-1.076010E 03
J= 2.5	-9.637283E 02	-1.084607E 03
J= 3.5	-9.734321E 02	-1.096843E 03
J= 4.5	-9.904810E 02	-1.112114E 03
J= 5.5	-1.008825E 03	-1.131028E 03
J= 6.5	-1.030614E 03	-1.153378E 03
J= 7.5	-1.055700E 03	-1.179162E 03
J= 8.5	-1.084134E 03	-1.208382E 03
J= 9.5	-1.115915E 03	-1.241037E 03
J=10.5	-1.151045E 03	-1.277127E 03
J=11.5	-1.189525E 03	-1.316652E 03
J=12.5	-1.231356E 03	-1.359603E 03
J=13.5	-1.276539E 03	-1.405988E 03
J=14.5	-1.325074E 03	-1.455802E 03
J=15.5	-1.376966E 03	-1.509046E 03
J=16.5	-1.432209E 03	-1.565717E 03
J=17.5	-1.490811E 03	-1.625816E 03
J=18.5	-1.552770E 03	-1.689337E 03
J=19.5	-1.618088E 03	-1.756285E 03
J=20.5	-1.686765E 03	-1.826653E 03
J=21.5	-1.758804E 03	-1.900445E 03
J=22.5	-1.834205E 03	-1.977657E 03
J=23.5	-1.912968E 03	-2.058289E 03
J=24.5	-1.995096E 03	-2.142339E 03
J=25.5	-2.080590E 03	-2.229807E 03
J=26.5	-2.169449E 03	-2.320691E 03
J=27.5	-2.261677E 03	-2.414991E 03
J=28.5	-2.357272E 03	-2.512706E 03
J=29.5	-2.456236E 03	-2.613833E 03
J=30.5	-2.558571E 03	-2.718374E 03
J=31.5	-2.664276E 03	-2.826327E 03
J=32.5	-2.773354E 03	-2.937690E 03
J=33.5	-2.885803E 03	-3.052464E 03
J=34.5	-3.001627E 03	-3.170647E 03
J=35.5	-3.120824E 03	-3.292239E 03
J=36.5	-3.243397E 03	-3.417238E 03
J=37.5	-3.369344E 03	-3.545646E 03
J=38.5	-3.498668E 03	-3.677459C 03
J=39.5	-3.631369E 03	-3.812679C 03
J=40.5	-3.767447E 03	-3.951304E 03

$v' = 0$, $A\ ^2\Sigma$ State

	$F_1(J'')$	$F_2(J'')$
J= 0.5	4.514898E 04	4.515296E 04
J= 1.5	4.515296E 04	4.516091E 04
J= 2.5	4.516091E 04	4.517284E 04
J= 3.5	4.517284E 04	4.518874E 04
J= 4.5	4.518874E 04	4.520862E 04
J= 5.5	4.520862E 04	4.523247E 04
J= 6.5	4.523247E 04	4.526030E 04
J= 7.5	4.526030E 04	4.529211E 04
J= 8.5	4.529211E 04	4.532788E 04
J= 9.5	4.532788E 04	4.536764E 04
J=10.5	4.536764E 04	4.541137E 04
J=11.5	4.541137E 04	4.545908E 04
J=12.5	4.545908E 04	4.551076E 04
J=13.5	4.551076E 04	4.556642E 04
J=14.5	4.556642E 04	4.562605E 04
J=15.5	4.562605E 04	4.568966E 04
J=16.5	4.568966E 04	4.575725E 04
J=17.5	4.575725E 04	4.582881E 04
J=18.5	4.582881E 04	4.590435E 04
J=19.5	4.590435E 04	4.598386E 04
J=20.5	4.598386E 04	4.606734E 04
J=21.5	4.606734E 04	4.615481E 04
J=22.5	4.615481C 04	4.624625E 04
J=23.5	4.624625E 04	4.634166E 04
J=24.5	4.634166E 04	4.644105E 04
J=25.5	4.644105E 04	4.654442E 04
J=26.5	4.654442E 04	4.665176E 04
J=27.5	4.665176E 04	4.676307E 04
J=28.5	4.676307E 04	4.687837E 04
J=29.5	4.687837E 04	4.699764E 04
J=30.5	4.699764E 04	4.712088E 04
J=31.5	4.712088E 04	4.724810E 04
J=32.5	4.724810E 04	4.737929E 04
J=33.5	4.737929E 04	4.751446E 04
J=34.5	4.751446E 04	4.765361E 04
J=35.5	4.765361E 04	4.779673E 04
J=36.5	4.779673E 04	4.794383E 04
J=37.5	4.794383E 04	4.809490E 04
J=38.5	4.809490E 04	4.824995E 04
J=39.5	4.824995E 04	4.840897E 04
J=40.5	4.840897E 04	4.857197E 04

$v'' = 1$, $X\ ^2\Pi$ State

	$F_1(J'')$	$F_2(J'')$
J= 0.5	-2.826695E 03	-2.946809E 03
J= 1.5	-2.831659F 03	-2.951713E 03
J= 2.5	-2.839932E 03	-2.959218E 03
J= 3.5	-2.851515E 03	-2.972124E 03
J= 4.5	-2.866408E 03	-2.987435E 03
J= 5.5	-2.884611E 03	-3.008146E 03
J= 6.5	-2.906126E 03	-3.028256F 03
J= 7.5	-2.930952F 03	-3.053767E 03
J= 8.5	-2.959091E 03	-3.082877E 03
J= 9.5	-2.990543E 03	-3.114985E 03
J=10.5	-3.025309E 03	-3.150691E 03
J=11.5	-3.063390E 03	-3.189792E 03
J=12.5	-3.104787C 03	-3.232291E 03
J=13.5	-3.149501E 03	-3.278183E 03
J=14.5	-3.197533E 03	-3.327469E 03
J=15.5	-3.248885E 03	-3.380148E 03
J=16.5	-3.303556E 03	-3.436217E 03
J=17.5	-3.361549E 03	-3.495677E 03
J=18.5	-3.422865E 03	-3.558526E 03
J=19.5	-3.487503F 03	-3.624764C 03
J=20.5	-3.555467E 03	-3.694388E 03
J=21.5	-3.626756E 03	-3.767398F 03
J=22.5	-3.701372E 03	-3.843793E 03
J=23.5	-3.779316E 03	-3.923571E 03
J=24.5	-3.860589E 03	-4.006732C 03
J=25.5	-3.945193E 03	-4.093275E 03
J=26.5	-4.033126E 03	-4.183195E 03
J=27.5	-4.124391E 03	-4.276500E 03
J=28.5	-4.218988E 03	-4.373180C 03
J=29.5	-4.316922E 03	-4.473247C 03
J=30.5	-4.418186E 03	-4.576676E 03
J=31.5	-4.522793E 03	-4.683488E 03
J=32.5	-4.630730C 03	-4.793680E 03
J=33.5	-4.742005E 03	-4.907246E 03
J=34.5	-4.856621E 03	-5.024176C 03
J=35.5	-4.974574E 03	-5.144484C 03
J=36.5	-5.095867E 03	-5.268168E 03
J=37.5	-5.220496E 03	-5.395219E 03
J=38.5	-5.348469E 03	-5.525644E 03
J=39.5	-5.479785E 03	-5.659438E 03
J=40.5	-5.614441E 03	-5.796602E 03

$v' = 1$, $A\ ^2\Sigma$ State

	$F_1(J'')$	$F_2(J'')$
J= 0.5	4.749086E 04	4.749480E 04
J= 1.5	4.749480E 04	4.750267E 04
J= 2.5	4.750267E 04	4.751448E 04
J= 3.5	4.751448E 04	4.753022E 04
J= 4.5	4.753022E 04	4.754990E 04
J= 5.5	4.754990E 04	4.757352E 04
J= 6.5	4.757352E 04	4.760107E 04
J= 7.5	4.760107E 04	4.763256E 04
J= 8.5	4.763256E 04	4.766798E 04
J= 9.5	4.766798E 04	4.770734E 04
J=10.5	4.770734E 04	4.775064E 04
J=11.5	4.775064E 04	4.779787E 04
J=12.5	4.779787E 04	4.784904E 04
J=13.5	4.784904E 04	4.790414E 04
J=14.5	4.790414E 04	4.796318E 04
J=15.5	4.796318E 04	4.802616E 04
J=16.5	4.802616E 04	4.809307E 04
J=17.5	4.809307E 04	4.816392E 04
J=18.5	4.816392E 04	4.823870E 04
J=19.5	4.823870E 04	4.831742E 04
J=20.5	4.831742E 04	4.840008E 04
J=21.5	4.840008E 04	4.848667E 04
J=22.5	4.848667E 04	4.857720E 04
J=23.5	4.857720E 04	4.867166E 04
J=24.5	4.867166E 04	4.877006E 04
J=25.5	4.877006E 04	4.887240E 04
J=26.5	4.887240E 04	4.897867E 04
J=27.5	4.897867E 04	4.908888E 04
J=28.5	4.908888E 04	4.920302E 04
J=29.5	4.920302E 04	4.932110E 04
J=30.5	4.932110E 04	4.944312E 04
J=31.5	4.944312E 04	4.956907E 04
J=32.5	4.956907E 04	4.969896E 04
J=33.5	4.969896E 04	4.983278E 04
J=34.5	4.983278E 04	4.997054C 04
J=35.5	4.997054E 04	5.011224E 04
J=36.5	5.011224E 04	5.025787E 04
J=37.5	5.025787E 04	5.040744E 04
J=38.5	5.040744E 04	5.056094E 04
J=39.5	5.056094E 04	5.071838E 04
J=40.5	5.071838E 04	5.087976E 04

TABLE II-2
FREQUENCY (cm^{-1}) (a), WAVELENGTH (Å) (b), AND HÖNL-LONDON FACTORS (c) FOR ROTATIONAL LINES OF THE (0,0) GAMMA BAND OF NO

V'= 0 V"= 6

P BRANCH

	11	12	21	22
J"= 1.5 J'= 0.5	44193.81 (a) 2282.77 (b) 0.402 (c)	44072.97 2266.86 1.848	44197.59 2262.57 0.550	44076.85 2266.76 1.900
J"= 2.5 J'= 1.5	44188.23 2262.99 1.631	44068.55 2268.20 2.094	44197.18 2262.59 0.647	44076.50 2266.79 2.276
J"= 3.5 J'= 2.5	44185.46 2263.19 1.845	44064.27 2269.41 2.459	44197.40 2262.58 1.278	44076.19 2268.86 2.805
J"= 4.5 J'= 3.5	44182.55 2265.35 2.275	44060.72 2269.60 2.788	44198.25 2262.55 1.672	44076.62 2268.78 5.591
J"= 5.5 J'= 4.5	44179.86 2263.47 2.928	44057.71 2269.75 5.122	44199.74 2262.46 2.035	44077.59 2268.75 4.015
J"= 6.5 J'= 5.5	44176.00 2263.57 5.605	44055.24 2269.68 5.457	44201.65 2262.55 2.571	44079.09 2268.65 4.870
J"= 7.5 J'= 6.5	44176.77 2265.65 4.307	44055.50 2269.98 2.729	44204.60 2262.21 2.861	44081.14 2268.54 5.555
J"= 8.5 J'= 7.5	44176.16 2263.66 5.022	44051.92 2270.65 3.999	44207.87 2262.04 2.966	44085.72 2268.41 6.065
J"= 9.5 J'= 8.5	44176.18 2262.66 5.781	44051.07 2270.09 4.247	44211.96 2261.63 3.227	44086.84 2266.25 8.801
J"=10.5 J'= 9.5	44176.84 2265.63 8.555	44050.75 2270.11 4.472	44218.59 2261.39 3.465	44090.51 2266.06 7.580
J"=11.5 J'=10.5	44178.11 2265.56 7.546	44050.99 2270.10 4.877	44221.84 2261.35 5.682	44094.72 2267.85 6.341
J"=12.5 J'=11.5	44186.01 2263.47 6.180	44051.77 2270.08 4.861	44227.72 2261.03 3.676	44099.47 2267.60 9.143
J"=12.5 J'=12.5	44182.54 2265.34 6.994	44055.09 2269.99 5.025	44234.22 2260.69 4.055	44104.77 2267.55 9.985
J"=14.5 J'=13.5	44165.89 2265.18 9.646	44054.96 2269.69 5.172	44241.35 2260.33 4.215	44110.62 2267.05 10.805
J"=15.5 J'=14.5	44169.49 2262.98 16.716	44057.38 2268.77 6.301	44249.09 2259.95 4.554	44117.61 2266.70 11.663
J"=16.5 J'=15.5	44195.84 2262.78 11.862	44060.34 2269.81 5.414	44257.45 2259.51 4.479	44123.85 2266.34 12.557
J"=17.5 J'=16.5	44186.85 2262.50 12.503	44062.85 2269.45 5.512	44266.44 2259.05 4.586	44151.43 2265.96 15.427
J"=18.5 J'=17.5	44204.46 2262.21 12.418	44667.91 2269.22 5.595	44276.04 2258.56 4.684	44139.47 2265.55 14.336
J"=19.5 J'=18.5	44210.72 2261.88 14.347	44072.52 2268.99 5.666	44286.26 2258.04 4.766	44148.06 2265.10 15.247
J"=20.5 J'=19.5	44217.58 2261.54 15.289	44077.69 2268.72 5.724	44297.09 2257.48 4.858	44157.20 2264.64 18.177
J"=21.5 J'=26.5	44225.05 2261.16 18.241	44085.41 2268.43 5.771	44306.54 2256.96 4.895	44166.80 2264.14 17.117
J"=22.5 J'=21.5	44253.14 2266.75 17.204	44089.68 2268.10 5.808	44320.60 2256.29 4.645	44177.15 2263.61 16.068

V'= 0 V"= 0

P BRANCH

	11	12	21	22
J"=25.5 J'=22.5	44241.84 2280.30 16.176	44096.52 2267.75 5.625	44333.28 2255.64 4.962	44197.98 2263.06 19.029
J"=24.5 J'=23.5	44251.15 2279.83 19.158	44102.91 2267.37 5.852	44346.58 2254.97 5.012	44199.52 2262.48 19.996
J"=25.5 J'=24.5	44261.07 2279.32 20.147	44111.85 2266.98 5.863	44560.48 2254.26 5.034	44211.24 2261.87 20.976
J"=26.5 J'=25.5	44271.60 2278.78 21.145	44120.36 2266.55 5.867	44374.96 2255.52 5.049	44225.75 2261.25 21.961
J"=27.5 J'=26.5	44282.74 2278.22 22.146	44129.45 2266.06 5.865	44590.08 2252.76 5.057	44236.77 2260.56 22.952
J"=28.5 J'=27.5	44294.48 2277.62 25.155	44159.05 2265.57 5.654	44405.60 2251.96 5.058	44250.27 2259.87 23.950
J"=29.5 J'=28.5	44306.84 2276.99 24.169	44148.24 2265.04 5.839	44422.13 2251.13 5.058	44264.55 2259.15 24.953
J"=30.5 J'=29.5	44581.79 2276.52 25.189	44159.98 2264.49 5.820	44459.06 2250.27 5.048	44279.26 2258.59 25.981
J"=31.5 J'=30.5	44335.28 2275.84 26.212	44171.21 2263.91 5.796	44458.60 2249.56 5.635	44294.55 2257.81 26.972
J"=32.5 J'=31.5	44547.52 2274.92 27.239	44163.18 2263.56 5.768	44474.74 2246.47 5.018	44510.41 2258.61 27.990
J"=35.5 J'=22.5	44562.29 2274.17 28.276	44195.63 2262.67 5.757	44493.49 2247.52 4.998	44326.65 2255.97 29.010
J"=34.5 J'=55.5	44377.66 2253.38 29.364	44206.64 2262.00 5.705	44512.84 2246.54 4.975	44343.62 2255.11 30.025
J"=35.5 J'=54.5	44595.64 2252.57 30.340	44222.22 2261.31 5.667	44522.79 2245.54 4.946	44361.37 2254.21 31.056
J"=36.5 J'=35.5	44410.21 2251.73 31.579	44258.37 2260.66 5.828	44553.35 2244.50 4.920	44379.49 2253.29 32.087
J"=37.5 J'=56.5	44427.28 2250.86 22.420	44251.08 2259.83 5.587	44574.46 2243.44 4.689	44398.18 2252.54 52.116
J"=26.5 J'=37.5	44445.16 2249.98 55.462	44288.37 2259.06 5.544	44598.25 2242.34 4.836	44417.44 2251.27 34.151
J"=39.5 J'=26.5	44463.53 2249.03 34.507	44282.22 2258.24 5.500	44618.58 2241.22 4.821	44437.27 2250.56 35.165
J"=40.5 J'=59.5	44482.50 2246.67 35.552	44296.64 2257.41 5.454	44641.52 2246.07 4.788	44457.67 2249.52 36.221

TABLE II-2 (Continued)

V' = 0 V'' = 0

Q BRANCH

	11	12	21	22
J''= 0.5 J'= 0.5	44198.82 2262.81 0.000	44078.13 2268.70 0.000	44202.80 2262.31 0.000	44082.11 2268.49 0.000
J''= 1.5 J'= 1.5	44197.59 2262.57 0.228	44078.85 2268.78 0.899	44205.54 2262.16 1.848	44084.90 2268.35 0.977
J''= 2.5 J'= 2.5	44197.12 2262.59 1.090	44076.50 2268.79 2.035	44209.11 2261.98 2.451	44082.23 2268.15 2.341
J''= 3.5 J'= 3.5	44187.40 2262.58 2.143	44078.19 2262.80 2.281	44213.30 2261.78 3.251	44092.09 2267.98 3.603
J''= 4.5 J'= 4.5	44122.25 2262.53 3.296	44078.82 2266.78 3.790	44218.13 2261.52 4.013	44096.50 2227.75 4.875
J''= 5.5 J'= 5.5	44199.74 2262.48 4.529	44077.89 2268.73 4.546	44225.59 2261.24 4.727	44101.44 2267.50 5.162
J''= 6.5 J'= 6.5	44201.65 2262.55 5.626	44079.09 2266.65 5.240	44229.88 2260.93 5.392	44106.82 2267.22 7.531
J''= 7.5 J'= 7.5	44204.60 2262.21 7.181	44081.14 2268.54 5.877	44238.40 2260.58 8.008	44112.94 2266.91 8.925
J''= 8.5 J'= 8.5	44207.97 2262.04 8.591	44083.72 2268.41 5.462	44243.75 2260.21 5.675	44119.50 2268.57 10.368
J''= 8.5 J'= 9.5	44211.96 2261.63 10.051	44086.84 2268.25 6.998	44251.72 2259.20 7.092	44128.60 2268.21 11.249
J''=10.5 J'=10.5	44218.52 2261.52 11.520	44090.51 2268.08 7.423	44260.32 2259.36 7.575	44154.24 2265.21 13.572
J''=11.5 J'=11.5	44221.84 2261.33 13.115	44094.72 2267.65 7.925	44269.55 2258.89 2.008	44142.43 2265.59 14.948
J''=12.5 J'=12.5	44227.72 2261.05 14.712	44099.47 2267.60 8.325	44279.40 2258.39 8.400	44161.12 2264.95 12.520
J''=13.5 J'=13.5	44254.22 2260.69 16.350	44104.77 5287.33 2.664	44289.68 2557.85 6.753	44160.43 2264.67 16.210
J''=14.5 J'=14.5	44241.35 2260.55 18.027	44110.82 2267.05 9.005	44300.98 2257.29 9.089	44170.25 2263.97 19.898
J''=15.5 J'=15.5	44249.09 2259.92 19.739	44117.01 2266.70 9.291	44312.70 2256.69 9.551	44120.62 2263.44 21.817
J''=16.5 J'=16.5	44257.45 2256.51 21.485	44123.85 2266.34 9.544	44325.04 2256.06 9.599	44191.53 2262.26 23.571
J''=17.5 J'=17.5	44265.44 2259.05 23.282	44131.43 2265.88 9.765	44338.00 2255.40 9.818	44202.99 2262.29 25.155
J''=18.5 J'=12.5	44278.04 2258.54 25.068	44139.47 2265.55 9.957	44351.57 2254.71 10.005	44215.01 2261.88 28.968
J''=19.5 J'=19.5	44288.28 2258.04 28.902	44146.06 2265.10 10.122	44365.77 2255.99 10.168	44227.87 2261.03 28.207
J''=20.5 J'=20.5	44297.09 2257.48 28.740	44157.20 2564.64 10.263	44380.58 2253.24 10.305	44240.69 2250.36 30.871
J''=21.5 J'=21.5	44308.54 2256.90 30.842	44166.90 2264.14 10.380	44388.00 2252.45 10.420	44254.36 2259.88 32.557

V' = 0 V'' = 0

Q BRANCH

	11	12	21	22
J''=22.5 J'=22.5	44320.60 2258.28 52.346	44177.15 9263.81 10.478	44412.04 2251.64 10.513	44286.59 2258.94 34.464
J''=23.5 J'=23.5	44533.38 2255.24 54.489	44187.98 2383.08 10.559	44428.69 2250.20 10.587	44283.37 2258.18 36.281
J''=24.5 J'=24.5	44348.58 2254.97 32.409	44199.32 2262.42 10.610	44445.95 2249.92 10.644	44296.71 2257.40 32.336
J''=25.5 J''=25.5	44380.46 2254.26 38.387	44211.24 2261.67 10.652	44463.82 2249.02 10.684	44314.61 2256.59 40.298
J''=26.5 J'=26.5	44274.98 2253.82 40.339	44223.73 2261.23 10.679	44422.30 2248.08 10.709	44331.07 2255.75 42.272
J''=27.5 J'=27.5	44390.08 2252.76 42.326	44236.77 2260.56 10.292	44501.59 2247.12 10.721	44348.08 2254.89 44.260
J''=28.5 J'=28.5	44405.80 2251.98 44.323	44250.37 2259.87 10.665	44521.09 2246.15 10.721	44365.62 2254.00 48.282
J''=29.5 J'=29.5	44422.13 2251.13 46.353	44264.53 2259.15 10.683	44541.40 2245.10 10.709	44383.80 2253.07 48.274
J''=30.5 J'=30.5	44439.06 2250.27 48.383	44279.26 2258.39 10.863	44562.30 2244.05 10.586	44402.50 2252.13 50 298
J''=31.5 J'=31.5	44456.60 2249.36 50 382	44294.55 2257.61 10.834	44585.62 2242.97 10 658	44421.77 2251.15 52 326
J''=32.5 J'=32.5	44474.74 2248.47 52.416	44310.41 2256.81 10.598	44605.94 2241.85 10.619	44441.60 2250.14 54 565
J''=33.5 J'=33.5	44493.49 2247.52 54.463	44328.83 2255.97 10.552	44628.66 2240.71 10.573	44462.00 2249.11 56 412
J''=34.5 J'=34.5	44512.84 2246.54 56.514	44243.82 2255.11 10.501	44651.98 2232.54 10 521	44482.98 2248 05 58.464
J''=35.5 J'=35.5	44532.79 2245.54 58.670	44361.37 2264.21 10 444	44675.91 5238.54 10.464	44504.49 2246.96 60 522
J''=32.5 J'=32.5	44653.33 2244.50 60.632	44379.49 2253.29 10.362	44700.43 2237 11 10.401	44528.59 2245 85 62.688
J''=37.5 J'=37.6	44574.46 2243.44 62.898	44382.18 2252.34 10.515	44725.55 2235.26 10.334	44549 25 2244.71 64 853
J''=38.5 J'=38.5	44596.23 2242.34 64 768	44417.44 2251.37 10.245	44751.28 2234.57 10 282	44572.49 2243.54 68.725
J''=39.5 J'=39.5	44212.58 2241.22 66.841	44437.27 2250.38 10.171	44777.60 2233.26 10.188	44596 29 2242 34 68 799
J''=40.5 J'=40.5	44641.52 2240.07 68.918	44457.67 2248.33 10 094	44804 52 2231.92 10 111	44620.66 2241.11 70 877

TABLE II-2 (Concluded)

V' = 0 V" = 0

R BRANCH

	11	12	21	22
J"= 0.5	44302.60	44082.11	44210.55	44090.05
J'= 1.5	2362.31	2268.49	2351 80	2268.08
	0 370	0 000	0.360	0.000
J"= 1 5	44205.54	44084.90	44217.42	44096.82
J'= 3 5	2253 15	2266.35	2261.55	2267.74
	0.950	0.175	0.934	0.201
J"= 2.5	44209.11	44088.23	44225 01	44104 12
J'= 3 5	2251 96	2268.18	2261.12	2267.36
	1 516	0 365	1.392	0.687
J"= 3 5	44313 30	44092.09	44233.16	44111.97
J'= 4 5	2281.76	2267.98	2260.73	2266 96
	2 104	0.950	1.829	1 233
J"= 4 5	44216.13	44094.50	44241.22	44120.35
J'= 5.5	2261.52	2267.75	2260.30	2265.53
	2.713	1.336	2.230	1.830
J"= 3.5	44223.59	44101.44	44251.43	44129.27
J'= 6.5	3361.34	2267.50	2259.81	2266.07
	3.346	1.696	2.802	2.440
J"= 6 5	44229 66	44105.92	44261.49	44138.73
J'= 7.5	2260.93	2267.22	2259.30	2266.66
	4.003	2.033	3.945	2.090
J"= 7 5	44236.40	44112.94	44272.16	44148.72
J'= 8.5	2260 55	2266 91	2258.75	2265.07
	4.665	2 546	3.263	3.786
J"= 8 5	44343.75	44118.50	44283.50	44159.26
J'= 9 3	2280.31	2265.57	3258.18	2364.53
	5 392	2.636	3.555	4.473
J"= 9.5	44251.72	44128 60	44295.45	44170.33
J'=10.5	2259.60	2236.21	2257 57	2363.96
	6.131	2.904	3.622	5.203
J"=10.5	44260.32	44134.24	44308.03	44181.93
J'=11.5	2259 36	2265.61	2956.93	2262.37
	6 873	2.150	4.068	5.957
J"=11.5	44269 55	44142.43	44521.23	44124.11
J'=12.5	2258 69	2265.39	2252.25	2262.74
	7.646	3 373	4 287	6.734
J"=12.5	44279.40	44151.15	44335.06	44206 22
J'=13.5	2258.39	2364.85	2255.55	2262.09
	2.440	3.580	4.427	7.833
J"=13.5	44289.86	44160.43	44349.52	44220.07
J'=14.5	2257.85	2364.47	2254.82	2261.42
	9.253	3.763	4.666	8.351
J"=14.5	44300.96	44170 25	44364.59	44933.22
J'=15.5	2257.29	2263.97	2254 05	2960.71
	10.086	3.932	4.227	9.190
J"=15.3	44312.70	44180 82	44380.29	44248.20
J'=16.5	2256.89	2263.44	2253.35	2259.92
	10.834	4.082	4.970	10.046
J"=16.5	44325.04	44191.53	44396.50	44263 08
J'=17.5	2256.06	2262.88	2252.42	2259 23
	11.900	4.215	5 096	10.919
J"=17.5	44338.00	44202.92	44413 54	44278.53
J'=18.3	2255.40	2262.29	2251.57	2258.43
	12.681	4.333	5.206	11.808
J"=16.5	44351.57	44215.01	44431.09	44294.52
J'=19 5	2254.71	2261.68	2250.68	2257.62
	13.576	4.427	5.301	12.713
J"=19.5	44365.77	44227.67	44449.25	44311.06
J'=20.3	2253.99	2261.03	2249.76	2256.77
	14.485	4 527	5.383	13.630
J"=20.5	44380.58	44240.60	44468 04	44328.15
J'=21.5	2255.24	2260.36	2248.21	2256.60
	15.408	4.608	5.451	14.561
J"=21.5	44396.00	44254.38	44487.44	44345.20
J'=22.5	2252.45	2259.66	2247.63	2255.00
	16 352	4.672	5.509	15.503

V' = 0 V" = 0

2 BRANCH

	11	12	21	22
J"=22.6	44412.04	44266.59	44507.46	44264.00
J'=23.5	2351.64	2256.84	2246.81	2264.09
	17.965	4.796	5.555	13.456
J"=23.5	44426.69	44283.37	44528.06	44382.76
J'=24.5	2250.80	2258.12	2246.77	2263.13
	18 235	4.774	5.591	17.418
J"=24.5	44445.95	44292.71	44549.32	44403.08
J'=25.5	2249.92	2257.40	2244.70	2262.15
	19.199	4.811	5.818	18.391
J"=25.5	44463.52	44314.51	44571.16	44421.85
J'=26.5	2249.02	2256.59	2243.60	2231.14
	20.169	4.840	5.638	19.373
J"=26.6	44482.30	44331.07	44593.63	44449.38
J'=27.5	2248.08	2255.75	2242.47	2260.10
	21.147	4.862	5.649	20.360
J"=27.5	44501.39	44346.08	44616.89	44463.38
J'=28.5	2247.12	2254.82	2241.21	2242.04
	22.133	4.876	5.654	21.355
J"=28.5	44521.09	44365.86	44640.36	44484.83
J'=29 5	2246.13	2254.00	2240.15	2247.95
	23.124	4.885	5.652	23.357
J"=29.5	44541.40	44383.80	44664.64	44507.04
J'=30.5	2245.10	2253.07	2238.91	2242.84
	24.191	4.227	5.645	23.324
J"=30 5	44562.30	44402.80	44682.52	44529.72
J'=31.5	2244.05	2253.13	3237.86	2245.69
	25.123	4.265	5.632	24.376
J"=31.5	44583.82	44421.77	44715.02	44552.28
J'=33.5	2242.97	2261.16	2236.39	2244.53
	25.130	4.878	5.815	25.393
J"=39.5	44605.84	44441.60	44741.11	44376.77
J'=33.5	2241.85	2250.14	2235.08	2343.32
	27.141	4.886	5.994	28.414
J"=55.5	44622.62	44469.00	44767.20	44601.14
J'=34.5	3240 71	2248.11	2233.75	2242.09
	28.156	4.851	5.568	27.439
J"=34.5	44851.96	44482.96	44785.10	44626.08
J'=35.5	2939.54	9248.05	2232.39	2240.34
	29.176	4.833	5.540	28.467
J"=35.5	44675 91	44504.49	44823.00	44631.59
J'=36.5	2238.34	3246.96	2231.00	2239.56
	30.195	4.811	5.509	29.498
J"=36.5	44700.43	44526.59	44281.50	44577.46
J'=37.5	2237.11	2345.85	2229.58	2238.23
	31.220	4.787	5.472	30.631
J"=37.5	44725.55	44549.25	44880.80	44704.30
J'=38.5	2335.86	2944.71	2228.13	2236.92
	32.246	4.760	3.440	31.567
J"=36.5	44751.28	44572.49	44910.30	44731.51
J'=39.5	2234.57	2242.54	2226.66	2235.56
	33.275	4.731	6.402	32.605
J"=39.3	44777.60	44598.29	44840.60	44759.29
J'=40.3	2233.25	2242.34	2223.12	2234.17
	34.305	4.701	3.362	33.644

UNCLASSIFIED

Security Classification

DOCUMENT CONTROL DATA - R & D

(Security classification of title, body of abstract and indexing annotation must be entered when the overall report is classified)

1 ORIGINATING ACTIVITY (Corporate author)	2a. REPORT SECURITY CLASSIFICATION
Arnold Engineering Development Center Arnold Air Force Station, Tennessee 37389	UNCLASSIFIED
	2b. GROUP N/A

3 REPORT TITLE

RESONANCE LINE ABSORPTION METHOD FOR DETERMINATION OF NITRIC OXIDE CONCENTRATION

4 DESCRIPTIVE NOTES (Type of report and inclusive dates)

Final Report

5 AUTHOR(S) (First name, middle initial, last name)

W. K. McGregor and J. D. Few, ARO, Inc., and C. D. Litton, UTSI

6 REPORT DATE	7a. TOTAL NO OF PAGES	7b NO OF REFS
December 1973	64	19

8a CONTRACT OR GRANT NO	9a. ORIGINATOR'S REPORT NUMBER(S)
b. PROJECT NO	AEDC-TR-73-182
c. Program Element 65802F	9b OTHER REPORT NO(S) (Any other numbers that may be assigned this report)
d.	ARO-ETF-TR-73-113

10 DISTRIBUTION STATEMENT

Approved for public release; distribution unlimited.

11 SUPPLEMENTARY NOTES	12 SPONSORING MILITARY ACTIVITY
Available in DDC.	Arnold Engineering Development Center, Arnold Air Force Station, Tennessee 37389

13. ABSTRACT The details of the derivation of working equations for the determination of the concentration of nitric oxide for measurement of the absorption of individual spectral lines lying between 2270 and 2260 Å in the NO (0,0) γ-band are presented. It is shown experimentally that the derivation is accurate, that published values of oscillator strengths are adequate, and that measurements of number densities with uncertainty no greater than ±20 percent are possible when proper corrections for the relative line widths of source and absorber are made. The density range of use of the (0,0) γ-band is from about 10^{14} to 10^{16} cm^{-3} for path lengths usually encountered in combustion system testing (10 to 100 cm). Extension of the range to larger concentrations by use of the (0,1) γ-band and the application to media having non-uniform concentration and temperature are discussed.

DD FORM 1 NOV 65 1473

UNCLASSIFIED

Security Classification

14. KEY WORDS	LINK A		LINK B		LINK C	
	ROLE	WT	ROLE	WT	ROLE	WT
absorption spectra						
band spectra						
combustion efficiency						
concentration						
nitrogen oxide						

AFSC
Arnold AFS Tenn